We thank the editor and reviewers for the comments to improve the quality of our manuscript. We have carefully addressed the comments with point-by-point replies to the editor and reviewers (in blue) and revised our manuscript accordingly. Attached is a marked-up version of the manuscript.

Reply to editor comments:

Editor comments to the author:
When revision your manuscript, please pay particular attention to the following aspects:
- Both referees comment on the use of snow depth of SWE. This is a critical issue. It is important to realize and recognize that snow depth is not a conservative quantity, and that there is a risk for bias when comparing snow depth observations between places with different microclimate conditions. This does not mean that there is no value in making a model based on snow depth observations, but the right arguments should be used to motivate this choice. This is not to reduce "any potential error when converting measured HS values to SWE." as is stated in the manuscript. The real reason (I guess) is that SWE observations are not available because they require more effort in sampling. But that does not make them less relevant. So please be clear in motivating the choices, and acknowledge any potential limitation and the fact that all models will use SWE and not snow depth.

You are right. We chose to parameterize snow depth over SWE because snow depth was spatially measured on the ground and not SWE. We could have applied an empirical new snow parameterization to derive spatial SWE based on e.g. interpolated air temperatures (as e.g. in Moeser et al., 2015b). This would however have introduced more uncertainty in an interception model since this is determined by the applied empirical density parameterization, measurement errors in air temperatures as well as by the spatial interpolation of temperatures. Converting snow depth to/from SWE with a density parameterization and its connected uncertainties thus remain controlled by the snow module (as part of a complex model) and these uncertainties will not be linked with the presented snow interception model.

We made the reasons why we chose snow depth over SWE for our interception models more clear (Section “Subgrid parameterization for forest canopy interception”).

- The choice for the functional relationships that are fitted to be data need to be motivated, and if possible evaluated against alternative models. There should be some objective criteria behind the choice for a particular functional form.

All parameterizations were empirically developed using the Swiss development data set. The existence of varying previously observed functional relationships (base functions) were mentioned in the introduction (Line 44-66) and were considered here. In the results section (276-279 and Line 283-291) we explain the reasoning for our functional relationship. In the discussion (Line 363-382) we largely discuss our choice compared to previously published base functions.

To specify the robustness of our regression coefficients we now included the confidence interval of the coefficients. Clearly, more spatial snow depth interception data sets would be advantageous. However, our empirical parameterizations are based on a development data set that is currently probably the most extensive existing data set available for spatial snow depth interception. This and the overall good performance of the parameterizations for the validation data set are reassuring that the models can be applied by various model applications. This is newly mentioned in the discussion.

- Please pay particular attention to the writing. If possible, let the manuscript be proof-read by a native speaker/colleague.
The manuscript was carefully read by several native English speakers from the USGS. The language was thus carefully checked before submission. Nevertheless, we went carefully through the manuscript again, and made the wording and structure more concise where appropriate.

Additional introduced changes by the authors:

1) For the revised manuscript, we decided to use the latest version of our code for computing the sky view factors, as this includes an improved visibility algorithm. This and the change that we now use σ_z in cm in all equations to be conform with the applied units for snow depth resulted in some changes in the regression coefficients. However, only very minor changes result in the figures and the performance table.

2) Furthermore, to avoid infinity for an extreme value of $\sigma_z=0$ in the parameterization of the standard deviation of snow interception (Eq. (4)) but keeping the functional form we introduced $\sigma_{HS}=f(1/(1+\sigma_z))$. This slight change in the functional form has almost no impact on modeled interception values and also changed performances only slightly.

The overall outcome of our work was not affected by these additional changes.

Reply to reviewer1 comments :

We thank the reviewer for their encouraging and constructive comments. Their comments (in italics) are addressed below. Answers to the reviewer are given in blue.

Major comments:

Throughout the paper forest structure is parameterized from a Digital Surface Model (DSM). If I am reading this correctly this is a DSM that is normalized to terrain to give a DSM in terms of vegetation height? (Z-axiz of Figure 2)? To be consistent with literature this should rather be termed a canopy height model (CHM) rather than a DSM. https://www.earthdatascience.org/courses/earth-analytics-python/lidar-rasterdata/lidar-chm-dem-dsm/

We parameterize forest structure from a Digital Surface Model (DSM) which is the top of the surface (as defined in the short course definition in https://www.earthdatascience.org/courses/earth-analytics-python/lidar-raster-data/lidar-chm-dem-dsm/), i.e. CHM+DTM.
You are right the caption of Figure 2 was unclear. We changed that and also stress in the introduction that canopy structure metrics are derived from DSM's.

Can you clarify the type of model you are presenting in context of the existing models? There was much discussion of other existing models and a clear compare/contrast of what you are presenting would be beneficial. This is simple empirical relationship with 1 or two input variables rather than a physical/mechanistic parameterization. This is critical to clarify so that future users can determine how to use this moving forward.
We agree that it is important to characterize the type of model. We added "empirical" when we refer to model throughout the manuscript to make this more clear: e.g. in the abstract: "We present two novel empirical models …", in the discussion: "We proposed two empirical models for.." resp. "We have derived just one empirical model for the standard deviation of snow interception.-.." and in the conclusion: "The empirical models integrate forest parameters..".

A clearer description of what was being measured at the various sites is needed. It was not immediately apparent that all of this was based on snow depth difference only and ignored density. The assumption that density of new snow accumulation is the same between open and forested areas is critical. Is it reasonable to assume that the standard error of 9.31 kg/m2 of new snow estimates is greater than observed snow density differences between open and forested? Even immediately after snowfall events there will be differences in density associated with unloading/compaction on the dripline of tree crowns versus the influence of blowing snow redistribution/erosion or not in clearings? At these locations is it reasonable to assume snowfall is the same between forest and clearing locations – any preferential deposition patterns evident? Variable blowing snow deposition/erosion in clearings versus forests? In the end do you have any observations that you could demonstrated that density differences are negligible or provide these values in terms of SWE? Any errors in density differences could lead to relatively large errors in interception ratios, especially for small events, and this needs to be clarified.

We agree that snow densities can be quite different between open and forested sites, especially with compaction and redistribution of snow by wind. Therefore we chose to parameterize snow depth and not snow water equivalent (SWE), which would require empirical parameterizations for the snow density itself (see Section 3.2 Subgrid parameterization for forest canopy interception). Until now we do not have available spatial, reliable SWE measurements comparable to the data set used in this study.

Note that the Swiss data was immediately acquired following a new snow fall event such that the influence of unloading, compaction and an eventual wind impact on the snowpack can be assumed reasonably small (see Moeser et al, 2015b).
In France, snow depth data was collected within a few days after the snow fall. The operational flat field site in France shows low wind speed and has therefore only very limited snow drift. Average hourly wind speed (at 10m height) is 1.2m/s over a period of 1993-2011 (Morin et al., 2012).
The open field site in the US may have been influenced by wind redistribution and compacting that might have created differences in the snowpack.

However, the data set from France and the US were only used as independent validation data sets, and the results are promising.

We improved the data description where we make clear that we used observed snow depth differences, i.e. independent measurements.

The transferability of this model is tested by applying the Swiss parametrization to French and US sites. While results are promising for between these sites I would temper some of the speculation (339-353). Relative to the large range of climatic conditions of cold-regions forests globally these sites represent relatively warm locations. As expressed elsewhere there has been variability in interception model performances between maritime and continental locations not to mention more temperature cold regions versus cold arctic treeline/tundra locations. Before recommending this for universal and widespread applications this model should be tested if possible at other locations that represent more end members.
While we agree that the novel models should be tested for a broad range of climatic conditions including extreme climate conditions and at various geographic sites we believe that the three sites already cover substantial variability (as shown by mean air temperatures and precipitation sums). We therefore believe that the novel models could perform sufficiently well in other climate conditions (though of course extremes have to be investigated). At the moment we do not have more snow interception data sets available that would allow an extended evaluation.

Note however, that we also point out the limitations of the models when applied for a deciduous forest. This was discussed in line 441-454.

We rephrased the section which now also more clearly mentions the limitations to soften our recommendation (395-415).

The approach implemented is to parameterize an empirical relationship. This will not work perfectly for all scenarios/locations obviously. Is it possible to quantify the uncertainty of the parameters and how they may vary between sites / vegetation types? How stable are these parameters?

Yes, our approach is to parameterize an empirical relationship. This model was then validated with independent data sets at different locations and for one different vegetation type, suggesting that it is also applicable in different climates/forests. Nevertheless, it is clear that more data is required to confirm this. To specify the robustness of our fitted parameters we included the confidence interval of the estimates.

Specific comments:
First sentence on abstract and line 19-21 are a little contradictory.
This was modified.

26-33: Transition to discussing surface albedo is abrupt. While snow interception/albedo is a critical feedback it is not extensively discussed hereafter? Can this section be simplified?
We agree and we rephrased the transition.

41-42: Awkward sentence
Agreed, we rephrased this sentence.

102: define more clearly what indirect interception measurements are.
Indirect interception measurements were introduced in line 36-38 in the introduction. We expanded the explanation in the data section as well.

151-154: what may the influence of different point cloud densities be upon the CHM derivation? Are there any recommendations you could make on what should be collected in future for proper a parameterization of your models?
In general the higher the point cloud, the greater the potential detail of the model. Specifically, if multi-return LiDAR is being integrated, then the higher the density of the last returns, the higher the potential detail of the DSM. This translates into a higher resolution CHM as well, since this data is subtracted from the raw data to create canopy heights from elevations.

1-m resolution DSMs computed from points clouds above 5 returns/m^2 are usually quite consistent, and are generally considered as suitable from automated tree detection. Local artifacts (NA or low pixels) can be expected due to heterogeneous scanning pattern on the ground, and to canopy penetration variability depending on forest type and beam intensity and divergence. But the description of the canopy at 1 m resolution is quite robust for such densities. Higher densities are probably required in the case of deciduous species with LiDAR data acquired in leaf-off conditions.
Ten years ago, country-wide acquisitions would be typically between 0.5 to 2 returns/m^2. Current available or scheduled country-wide datasets are now around 1-5 returns/m^2 (e.g., Denmark 5 returns/m^2, North-Rhine Westphalia in Germany 4 returns/m^2, Spain 1 return/m^2, France 2 to 5 returns/m^2).
We can expect that thanks to technical improvements in LiDAR sensors, the density of 5 returns/m^2 will be exceeded in most countrywide campaigns in the next decade. Besides, acquisitions over smaller areas (municipalities…) have usually higher densities.

205: how are you getting from SP at a point to mean sky view factor. How is the space being discretized? Are you computing SP on a fine scale grid and averaging values over a coarser scale of interest?

Here, we derive the sky view factor *F*sky using Eq. (1) for each fine-scale grid cell in a DSM. A spatial mean is obtained by averaging all fine-scale grid cells within a coarse-scale grid cell. The spacing thus depends on the available fine-scale grid cell resolution of the DSM. We do not use *F*sky derived from SP. We made this clear in line 211-219.

248-250: can you clarify this reversed response?
Deriving the sky view factor *F*sky using Eq. (1) for a fine-scale grid cell in a DSM implies a calculation on the DSM. Deriving *F*sky from HP or SP allows a view from below canopy. Since we do not use HP derived *F*sky and to avoid confusion we removed the second part of the explanation.

279: Why do we want to know the standard deviation of snow interception. Can you articulate a broader reason to calculate this?
While we had some explanations at the end of the introduction we added some at the beginning of Section 3.2.

286-287: As canopy gets to be more homogeneous the spatial variability of interception increases? How?
The larger σ_z the more trees are in a field area (50x50m^2 plot), i.e. the denser the coverage:

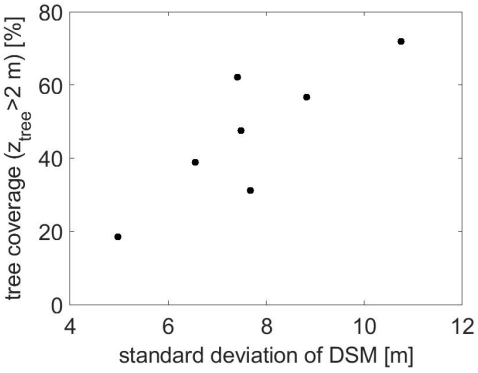

Based on our data set larger σ_z implies larger spatial mean interception, but lower spatial variability of interception. Lower σ_z implies lower spatial mean interception, but larger spatial variability of interception:

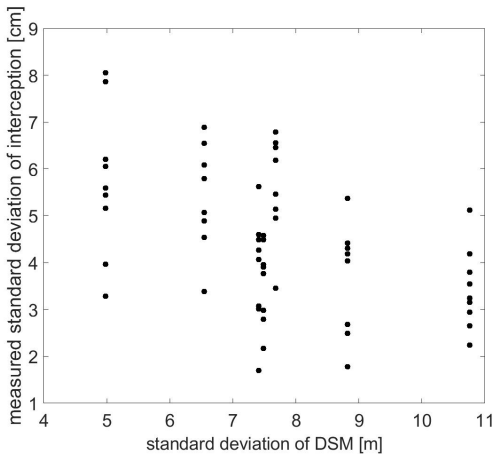

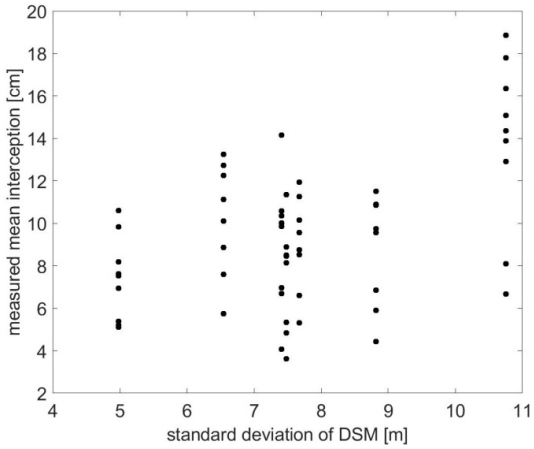

We will rephrase the explanation in line 320-323.

To avoid infinity for an extreme value of σ_z=0 but keeping the functional form we introduced σ_{HS}=*f*(1/(1+σ_z)). This new form changes modeled interception values and performances only slightly. We changed this in the revised manuscript.

322-324: Could a global product (between 51.6_ N and 51.6_ S at least) for these metrics
be derived from the GEDI platform? https://gedi.umd.edu/
Thanks a lot for pointing us towards the GEDI platform. This is a very promising mission. A GEDI product exists with 25 m grid resolution for ground elevation and canopy top height (L1A-2A). We assume a product like thus could be used to compute *F*sky spatially (Eq. (1)).

However, a 25 m fine-scale DSM is much coarser than the resolutions used here for developing a snow interception model. This might need a scale-dependent investigation.

365: Typo "ASifferences"
Corrected.

381-383: Deciduous will have very different behavior than coniferous vegetation. Could you reoptimise your model for deciduous specific sites? Would be interesting to know if the same scaling laws were applicable to know if a separate deciduous scaling parameterization is needed or not.
We agree that snow interception models should be verified for different vegetation species. As discussed in line 266- 270 Huerta et al. (2019) showed very recently that current interception models developed for coniferous vegetation required recalibrating of fit parameters to be applicable in deciduous forests. However, the same scaling laws were applicable.
Our models were developed and validated for coniferous vegetation. We further validated the models with indirect interception measurements from two measurement campaigns conducted in a deciduous forest in the US. Larger biases resulted. However, we could not perform a solid validation of our models with this data set since the LiDAR point cloud was acquired during leaves-on conditions, which led to overestimations in modeled interception.
To develop empirical interception models for deciduous forests measurement campaigns and a LiDAR acquired during leaves-off conditions are required.

386-388. Why? Can you justify this a bit more?
Unfortunately, it is not fully clear to us what your question is.
The novel interception models presented here, use forest structure metrics which can be derived spatially on a DSM without tedious field measurements. The accuracy of the derived metrics is dictated by the resolution of the DSM. In contrast a more accurate presentation of forest structure metrics might be achieved using field measurements (e.g. HP) but then a spatial coverage is not feasible.

412-416: The full summary of the various interception efficiencies would be better presented in the results rather than in the conclusion for the first time.
We prefer having this summary in the conclusions. It is not really a result, but rather characterizes observed snow interception in general compared to our datasets. It further confirms previously observed annual snow interception fractions which were mentioned at the beginning of the introduction.

423-425: long challenging sentence
We rephrased this sentence.

Figure 1: Can scale bars and north arrows be consistently sized and located on edge of orthophotos? Where snow depth measurement setups the same for each point in the respective sites?
Yes, the snow depth measurement setups were the same for each point in the respective sites. We made Figure 1 more consistent.

Figure 2: what is grid resolution of DSM (aka CHM)? What UTM zone is applicable for the respective easting/northing? Correct sig figs on the easting northing?
The coordinates of Figure 2 are displayed in the Swiss reference system CH1903+. It is metric similar to UTM. Grid resolution of the CHM's is 1 m as for the DSM's. This information was added to the caption.

Figure 4-6: "Parametrized" or "Modelled" interception on y-axis label
We changed the labels to "Modeled interception".

Reply to reviewer2 comments :

We thank the reviewer for their encouraging and constructive comments. Their comments (in italics) are addressed below. Answers to the reviewer are given in blue.

Major comments:

The language needs to be improved to be more concise. Just as one example: P1L17: Would snow in another season not be intercepted? Both in this sentence and the next one I assume the authors mean that in a coniferous forest 60% may be intercepted. As it reads now, 60% of some total are intercepted in coniferous forests and 24% are intercepted in deciduous forests in the Andes, i.e. 84% are retained in total. I agree that this is a minor detail and one can guess what the authors mean, but in a scientific paper these things should be formulated as clearly as possible.
The manuscript was carefully read by all co-authors and additionally by several native English speakers from the USGS. The language was carefully checked before the submission. Nevertheless, to we carefully went through the manuscript once more, and made the wording and structure more concise where appropriate.

Central parts of the methods are described first in the result section.
Unfortunately we do not fully understand which parts you mean. All methods are described in the methods section. The result section is structured as follows:

4.1. Grid cell mean snow interception
4.1.1 Parameterization
4.1.2 Validation

4.2 Grid cell standard deviation of snow interception
4.2.1 Parameterization
4.2.2 Validation

The resulting parameterizations should not be part of the methods section, they were newly developed in this study using the data given in the data section, the forest structure metrics and the method that are both described in the methods section (3.1 and 3.2). As such the parameterizations (i.e. 4.1.1. and 4.2.1) are part of the results. The validation sections (within in the results) describe how modeled interception compares to observed interception for the development and the validation data sets (i.e. 4.1.2. and 4.2.2).
While we do not see that parts of the results should be moved to the methods we agree that the headings could be more concise and we changed them to make the overall structure more clear.

The field observations need to be described in more detail. I honestly do not understand what has been measured how. It also sounds as if some data were selected from a larger set, the reasons for this are not entirely clear.
Unfortunately, we do not understand which data you think were selected from a larger set. However, we carefully went through the data section and clarified the description of the measurement methods where necessary.

The two central equations suddenly pop up in the result section. How were these two types of equations derived? Is there any physical reasoning for certain functional relationships like the exp or power function? How exact can the coefficients be determined? Uncertainty? Sensibility?
In the methods section
3.2 Subgrid parameterization for forest canopy interception
we describe that the empirical parameterizations are derived using the Swiss data set.

All parameterizations were empirically developed using the Swiss development data set. The existence of varying previously observed functional relationships (base functions) were mentioned in the introduction (Line 44-50) and were considered here. In the results section (268-269, 275-279 and 283-291) we explain the reasoning for our functional relationship. In the discussion (Line 363-388) we largely discuss our choice compared to previously published base functions.

To specify the robustness of our coefficients we now included the confidence interval of the regression coefficients and clearly discuss the need for more data in the discussion.

Furthermore, I do not understand what the stdev of the DSM is. Variation of ground surface? But this would not have anything to do with the trees. Variation of vegetation heights? But then DSM is the wrong term.
Forest structure is parameterized here from the Digital Surface Model (DSM) which is the top of the surface, i.e. surface elevation + vegetation height (DTM+CHM). DSM is a standard abbreviation for the surface height (e.g. https://www.earthdatascience.org/courses/earth-analytics-python/lidar-raster-data/lidar-chm-dem-dsm/). The abbreviation DSM was introduced in line 92.

The standard deviation of DSM σ_z describes the variation of vegetation altitude by integrating both the variability of the canopy height and of terrain elevation. Using σ_z seems more realistic because gaps and spaces between trees are influenced by local topography. The standard deviation of DSM σ_z was introduced in the methods section as our second forest structure metric (3 Methods / 3.1 Forest structure metrics last section).

We further investigated using the standard deviation of the CHM. For our data sets this didn't change the overall functional relationship. Furthermore, correlation coefficients were larger between mean snow interception and σ_z derived from DSM than between mean snow interception and σ_z derived from CHM. Since all data used in this study was however collected in rather flat field sites, this may have to be verified in steeper terrain. This is now discussed.

My major concern regarding usability is the choice to express everything as snow height rather than SWE. When used as part of a larger model, I would assume one is most often interested in SWE rather than heights. Also conceptually I am not sure what the height of intercepted snow implies? Height on branches? Probably rather height as the snow would be if being on the ground? But then at which density, that of the other snow on the ground or that of the intercepted snow? Sorry, but I find this very confusing and limiting. Thus, I would prefer to see the interception etc expressed in SWE.

We deliberately chose to parameterize snow depth over SWE because snow depth was spatially measured on the ground and not SWE.
We could have applied an empirical new snow parameterization to derive spatial SWE based on e.g. interpolated air temperatures (as e.g. in Moeser et al., 2015b). This would however have introduced a lot of uncertainty in an interception model since this is determined by the applied empirical density parameterization, measurement errors in air temperatures as well as by the spatial interpolation of temperatures. This was discussed in Section 3.2.
We therefore decided to derive spatial snow depth interception estimates from snow depth observations within and outside of the forest. Converting snow depth to/from SWE with a density parameterization and its connected uncertainties thus remain controlled by the snow module (as part of a complex model) and these uncertainties will not be linked with the presented snow interception model.

We largely expanded our explanation in Section 3.2.

As the two equations are derived from data for ideal situations (no prior snow …) I am not sure how these should be used for the real case, where there is often a history of prior snow on the trees. It seems here one might run into the problem that a simple empirical equation is not really a model after all.
You are right our parameterizations were developed on a data set that had no prior snow on tree branches when the precipitation event started. Nevertheless, both validation data sets did not have this prerequisite but still compared well to modeled interception using the novel empirically derived parameterizations. Especially the interception data set from the US often integrated snow interception over several storms due to longer time periods between data collection. Thus, the trees weren't necessarily snow free for a following snowstorm. Instead these measurements may have been influenced by snow settling, wind redistribution, sublimation, unloading and melt.
This was discussed in Line 424-426.

For a 'model' I would expect some canopy storage accounting, which is an aspect that is missed here.
We have focused on improvements of an interception model rather than multiple related processes. Modeling forest canopy involves several processes, each of which are described with separate models. This includes, unloading, melt and drip (some models), and sublimation. These models use the interception model to dictate how much snow is in the branches at any point in time. If there is still snow in the branches, then it is depleted by the unloading, melt and drip and sublimation models. Thus, canopy storage is dictated by the interplay of each individual model.

We discussed that we present a model for one forest process. To make this more clear we rephrased the explanation (Line 427-431). Furthermore, we made this clear in the method section: "3.2 Subgrid parameterization for forest canopy interception".

Snow processes in mountain forests: Interception modeling for coarse-scale applications

Nora Helbig[1], David Moeser[2], Michaela Teich[3,4], Laure Vincent[5], Yves Lejeune[5], Jean-Emmanuel Sicart[6], and Jean-Matthieu Monnet[7]

[1]WSL Institute for Snow and Avalanche Research SLF, Davos, Switzerland
[2]USGS, New Mexico Water Science Center, Albuquerque, U.S.
[3]Austrian Research Centre for Forests (BFW), Innsbruck, Austria
[4]Department of Wildland Resources, Utah State University, Logan, UT, U.S.
[5]Univ. Grenoble Alpes, Université de Toulouse, Météo-France, CNRS, CNRM, Centre d'Études de la Neige, Grenoble, France
[6]Univ. Grenoble Alpes, CNRS, IRD, Grenoble INP, Institut des Géosciences de l'Environnement (IGE) - UMR 5001, F-38000 Grenoble, France
[7]Univ. Grenoble Alpes, INRAE, LESSEM, F-38402 St-Martin-d'Hères, France

Correspondence: Nora Helbig, (norahelbig@gmail.com)

Abstract. Snow interception by forest canopy ~~drives the~~ controls spatial heterogeneity of subcanopy snow accumulation leading to significant differences between forested and non-forested ~~areas~~ sites at a variety of scales. Snow intercepted by forest canopy can also drastically change the surface albedo. As such, ~~accuratelly modelling~~ accurately modeling snow interception is of importance for various model applications such as hydrological, weather and climate predictions. Due to difficulties in direct measurements of snow interception, previous empirical snow interception models were developed at just the point scale. The lack of spatially extensive data sets has hindered validation of snow interception models in different snow climates, forest types and at various spatial scales and has reduced accurate representation of snow interception in coarse-scale models. We present two novel empirical models for the spatial mean and one for the standard deviation of snow interception derived from an extensive snow interception data set collected in a ~~spruce~~ coniferous forest in the Swiss Alps. Besides open ~~area snow fall~~site snowfall, subgrid model input parameters include the standard deviation of the DSM (digital surface ~~models) and~~model) and/or the sky view factor, both of which can be easily pre-computed. Validation of both models was performed with snow interception data sets acquired in geographically different locations under disparate weather conditions. Snow interception data sets from the Rocky Mountains, U.S., and the French Alps compared well to ~~modelled~~ modeled snow interception with a ~~NRMSE~~ Normalized Root-Mean-Square Error (NRMSE) for the spatial mean of $\leq$ 10 % for both models and NRMSE of the standard deviation of $\leq$ 13 %. Our results ~~suggest~~ indicate that the proposed snow interception models can be applied in coarse land surface model grid cells provided that a sufficiently fine-scale DSM ~~of the forest~~ is available to derive subgrid forest parameters.

1 Introduction

Snow interception is the amount of snow captured in the forest canopy. In winter as much as 60 % of the cumulative snowfall may be retained in conifer forests (Pomeroy and Schmidt, 1993; Pomeroy et al., 1998; Storck and Lettenmaier, 2002) and as much as 24 % of total annual snowfall may be retained in deciduous forests in the ~~Southern~~ southern Andes (Huerta et al., 2019). Due to the sublimation of intercepted snow, a large portion of this snow never reaches the ground (Essery et al., 2003) and the interplay of interception and sublimation creates significant ~~below forest~~ below-forest heterogeneity in snow accumulation. Rutter et al. (2009) estimated that 20 % of the seasonal snow cover ~~within~~ in the Northern Hemisphere is located within forested areas. As such, the mass balance of solid precipitation in forested regions, characterized by strong spatial variability of snow accumulation, is a large contributor to the global water budget. Accurately modeling the spatial distribution of snow water equivalent in forested regions is thus necessary for climate and water resource modeling over a variety of scales (see Essery et al., 2009; Rutter et al., 2009). ~~Surface albedo is a significant driver of the global surface energy balance and precise albedo estimations are critical for a range of model applications such as climate scenarios (Hall, 2004) . However~~Furthermore, intercepted snow can drastically change surface albedo values in forested regions. Previous studies observed large albedo differences (a range of 30 %) between snow-free and snow-covered forest stands (e.g. Roesch et al., 2001; Bartlett and Verseghy, 2015; Webster and Jonas, 2018). Thus, in mountainous areas where forested and alpine regions coexist, accurate estimates of forest albedo play a key role in correctly modeling the surface energy balance. Due to the connectivity between interception and albedo, formulations of surface albedo over forested areas necessitate estimates of intercepted snow (e.g. Roesch et al., 2001; Roesch and Roeckner, 2006; Essery, 2013; Bartlett and Verseghy, 2015).

So far, direct snow interception measurements have only been retrieved from weighing trees. These measurements are limited to the point scale, are resource intensive sampling and only allow for analysis of small to medium size trees, or tree elements (Schmidt and Gluns, 1991; Hedstrom and Pomeroy, 1998; Bründl et al., 1999; Storck and Lettenmaier, 2002; Knowles et al., 2006; Suzuki and Nakai, 2008). However, there are indirect techniques ~~which~~ that allow for estimations of interception over larger spatial scales. Indirect measurements that compare snow accumulation between open and forest sites allow for a larger spatial sampling~~but can~~ , but may be affected by other snow forest processes, such as ~~by~~ snow unloading. As such, sample timing of snow storm conditions needs to be evaluated ~~(e.g. Satterlund and Haupt, 1967; Schmidt and Gluns, 1991; Hedstrom and Pomeroy, 19~~ (e.g. Satterlund and Haupt, 1967; Schmidt and Gluns, 1991; Hedstrom and Pomeroy, 1998; Moeser et al., 2015b; Vincent et al., 2018) . Until recently, snow interception could not be ~~spatially acquired over spatial~~ characterized over length scales on the order of several tens of meters~~at which~~ . However, at these scales snow interception can spatially vary due to canopy heterogeneity. The extensive data set of indirect snow interception measurements in coniferous forests in eastern Switzerland of Moeser et al. (2015b) is probably the first data set that allows a thorough spatial analysis of snow interception.

Several statistical ~~parameterizations~~ models for forest interception ~~snow depth (I_{HS}) and snow~~ of snow water equivalent (I_{SWE}) have been suggested using a variety of canopy metrics and functional dependencies for the rate and amount of storm snowfall (e.g. Satterlund and Haupt, 1967; Schmidt and Gluns, 1991; Hedstrom and Pomeroy, 1998; Hellström, 2000; Lundberg et al., 2004; Andreadis et al., 2009; Moeser et al., 2015b; Huerta et al., 2019; Roth and Nolin, 2019). Though these

~~parameterizations~~ models have been demonstrated to perform well, they often rely on detailed forest canopy density and structure metrics ~~which~~ that are either not readily available or cannot easily be upscaled~~to larger scales~~, limiting functionality in models where the mean of model grid cells over several hundreds of meters to a few kilometers is required, i.e. potentially reducing validity in large scale modeling efforts.

Traditional forest metrics used to parameterize snow interception include leaf area index (LAI), canopy closure (CC) and canopy gap fraction (GF) or sky view. These are mainly derived from hemispheric photographs (HP) taken from the forest floor looking upwards. However, these indices can also be estimated from synthetic hemispheric photographs (SP). SP images mimic HP images but are generated from aerial LiDAR (light detection and ranging) data. This requires the inversion of LiDAR to a ground perspective and conversion from a Cartesian to a polar coordinate system (Moeser et al., 2014). Prior work has also used return density ratios of LiDAR, which is computationally faster but less accurate than SP images (Morsdorf et al., 2006). Canopy structure, or the position of a canopy element relative to the surrounding forest canopy, ~~have~~ has also been used to model snow interception. However, as pointed out by Moeser et al. (2015b), some forest structure metrics such as LAI and CC are highly cross-correlated. ~~Varhola et al. (2012) reviewed most of the currently employed forest canopy structure and density metrics.~~ Moeser et al. (2015b, 2016) expanded on prior interception models, which mostly rely on the highly cross-correlated traditional forest density parameters LAI and CC by introducing uncorrelated, novel forest structure metrics. Their empirical interception model utilizes total open area, mean distance to canopy and CC. While the latter parameter was derived from SP (Moeser et al., 2014), the first two parameters were directly computed from a ~~DSM~~digital surface model (DSM). Total open area is defined as the total open area in the canopy around a point, and mean distance to canopy defines how far away the edge of the canopy is from a point. ~~Very recently (Roth and Nolin, 2019)~~ Recently Roth and Nolin (2019) extended mean distance to canopy vertically, by deriving it for 1 m horizontal slices that were normalized with the corresponding elevation above the ground.

Due to the difficulties in measuring snow interception, previous empirical snow interception models were not validated in different snow climates, forest types or at varying spatial scales. During SNOWMIP2 (Essery et al., 2009; Rutter et al., 2009), where 33 snow models were validated at ~~single~~ individual forested as well as open sites, many models used the snow interception parameterization from Hedstrom and Pomeroy (1998). This interception model was one of the first that used canopy metrics (LAI and CC)~~. Though,~~ , although a snow interception model for larger scales also requires the greater canopy structure. Overall, SNOWMIP2 showed that maximum snow accumulation predictions ~~varied among the~~ had large errors compared to observed values in most models but snow cover duration was well estimated. Furthermore, a universal best model could not be found ~~since~~ because model performances at forest sites varied. This may explain why there is still no common ground with several snow-related variables in land surface models (Dirmeyer et al., 2006), which led to the current Earth System Model-Snow Model Intercomparison Project (ESM-SNOWMIP) showing overall larger errors in simulated snow depth on forest sites than on open sites (Krinner et al., 2018). Recently Huerta et al. (2019) validated three previous snow interception models developed for coniferous forests with observed point snow interception values in a deciduous southern beech- (*Nothofagus*~~ forest of the Southern~~ -) forest of the southern Andes. All three empirical models required recalibration, with the recalibrated Hedstrom and Pomeroy (1998) model showing the overall best performance. Similarly, model simulations of Vincent et al. (2018)

largely overestimated observed accumulated snow depth in a spruce forest at Col de Porte in the ~~Southeastern~~ southeastern French Alps. They attribute this to errors in the processes linked to the snow interception model based on Hedstrom and Pomeroy (1998) due to an underestimation of the melt of intercepted snow. Previous snow interception models also failed to accurately model snow interception ~~from~~ in a maritime climate ~~Roth and Nolin (2019)~~(Roth and Nolin, 2019). While Roth and Nolin (2019) successfully ~~modelled snow interception by including air temperature~~ modeled snow interception in a maritime climate, their model consistently ~~underestimates~~ underestimated snow interception in a continental climate forest. Overall, this demonstrates the need for more robust parameterizations of the processes affecting snow under forest, which is an important challenge for global snow ~~modelling~~modeling.

When modeling at resolutions greater than the point scale, accurate implementation of forest snow processes necessitates not just the mean of a grid cell but the standard deviation within a grid cell or model domain. However, to our knowledge, the standard deviation of snow interception has not yet been quantified. In this paper, we propose empirical parameterizations for the spatial mean and standard deviation of snow depth interception (I_{HS} and $\sigma_{I_{HS}}$) derived from indirect interception measurements at sites with length scales on the order of several tens of meters. We analyzed an extensive data set consisting of several thousand interception measurements collected immediately after storm events in a discontinuous coniferous forest stand in the ~~Eastern Swiss Alps (Moeser et al., 2014, 2015a, b, 2016)~~eastern Swiss Alps (Moeser et al., 2014, 2015a, b). From a LiDAR ~~digital surface model (DSM)~~ DSM with elevations z (Moeser et al., 2014), we derived two canopy structure metrics: (1) the standard deviation of the DSM (σ_z) in order to represent the spatial heterogeneity of ~~canopy~~ surface height in a forested model domain and (2) spatial mean sky view factor (F_{sky}), which roughly represents the spatial mean canopy openness but is derived here on the ~~Cartesian~~ DSM from geometric quantities that describe the received radiative flux fraction emitted by another visible surface patch (i.e. canopy patches) (Helbig et al., 2009). These two metrics were correlated to spatial means and standard deviation of the indirect interception measurements. We validated the novel ~~parameterizations~~ models with new indirect snow interception measurements from one site located in the Rocky Mountains of ~~Northern Utah, United States~~ northern Utah, U.S. and from one site located at Col de Porte in the ~~Southeastern~~ southeastern French Alps.

2 Data

In this study we solely used indirect snow depth interception measurements. Indirect snow interception data was obtained from comparing new snow depth accumulation between open and forest sites. This indirect technique allows for a collection of snow interception data over a larger area and finally also to investigate the spatial snow interception variability. We used three snow interception data sets: One, from the eastern Swiss Alps, for the development of snow interception models and two for the independent validation of the developed snow interception models from the Rocky Mountains of northern Utah in the U.S. and from the southeastern French Alps. In each data set snow interception was derived slightly different.

2.1 Eastern Swiss Alps

Indirect interception measurements were collected in seven discontinuous coniferous forest stands near Davos, Switzerland at elevations between 1511 m and 1900 m above sea level (a.s.l.) consisting of primarily Norway spruce (*Picea abies*) (Fig. 1a). Mean annual air temperature in Davos (1594 m a.s.l.) is approximately 3.5 °C and the average solid precipitation is 469 cm per year (climate normal 1981-2010, ~~MeteoSwiss~~https://www.meteoswiss.admin.ch). The field sites are maintained and operated by the Snow Hydrology group of the WSL Institute for Snow and Avalanche research SLF in Davos, Switzerland. The sites were chosen to limit influence of slope and topographic shading while capturing as much diversity as possible in elevation, canopy density and canopy structure (see canopy height models (CHM) of two field sites in Fig. 2). ~~Each of the seven field areas~~ All seven field sites were equipped in the same manner and consisted of 276 marked and georectified measurement points (about $\pm$50 cm) over a 250 m^2 surface area (yellow inlet in Fig. 1a corresponds to each yellow dot). Two non-forested reference sites (open field ~~area) reference siteswere also equipped~~ sites) (see blue dots in Fig. 1a) were equipped with 50 measurements points each to derive the ~~indirect snow interception measurements~~average open site snowfall (accumulated snowfall).

During the winters of 2012/2013 and 2013/2014, snow depth was measured ~~at all field points,~~ immediately after every storm with greater than 15 cm ~~of open area~~ depth of open site snowfall. In total, nine storm events met the following pre-storm and storm conditions that allowed for indirect interception measurements: (1) no snow in canopy prior to a storm event, (2) defined crust on the underlying snow, and (3) minimal wind redistribution during the storm cycle. New snow was measured down to the prior snow ~~layers crust to~~ layer crust from the top of the newly fallen snow layer to represent total snow ~~fall-snow~~ interception. Total ~~snow fall~~ snowfall was measured at the open field ~~areas.~~ sites. Snow interception was obtained by subtracting the total snowfall measured in the forest from the total snowfall measured at the open field site. The extensive measurement data set used in this study ~~was previously published~~ is described in high detail in ~~Moeser et al. (2014, 2015a, b, 2016). For this study, 13994 of the individual measurements were used to compute~~ Moeser et al. (2014, 2015a, b). Pre-processing resulted in 13'994 usable individual measurements from which 60 site based mean and standard deviation values of snow interception ~~, which~~ could be computed. These 60 values were then utilized to develop the interception parameterizations. For all individual measurements, a mean snow interception efficiency (interception / new snowfall open) of 42 % was measured with values ranging from 0 to 100 %. The probability distribution function (pdf) of all snow interception data can be fitted with a normal distribution (positive part) with a Root-Mean-Square Error (RMSE) of the quantiles between both distributions of 0.6 cm and a Pearson correlation r of 0.99 for the quantiles (Fig. 3). Average storm values of air temperatures covered cold (-12.1 °C) to mild (-1.9 °C) conditions.

A ~~1 m^2~~ 1-m resolution gridded LiDAR DSM was generated from a flyover in the summer of 2010 and encompasses all ~~field areas (~~eastern Swiss Alps field sites (see Fig. 1a for the extent). The initial point cloud had an average density of 36 points/m^2 (all returns) and a shot density of 19 points/m^2 (last ~~return~~returns only). The ~~1 m~~1-m^2 resolution LiDAR DSM is used for the derivation of the canopy structure metrics, the standard deviation of the DSM (σ_z) and the spatial mean sky view factor (F_{sky}) over each 50x50m^2 field site.

2.2 Rocky Mountains of ~~Northern~~ northern Utah~~in the United States~~, U.S.

For the first validation data set, indirect interception measurements were collected at Utah State University's T.W. Daniel Experimental Forest (TWDEF; 41.86°N, 111.50°W) that is located at ∼2700 m a.s.l. in the Rocky Mountains of ~~Northern~~ northern Utah (Fig. 1b). The forest stand is predominantly coniferous and is composed of Engelman spruce (*Picea engelmannii*) and subalpine fir (*Abies lasiocarpa*). However, ~~there are deciduous~~ deciduous quaking aspen (*Populus tremuloides*) forest stands ~~present. Modelled mean~~ are also present. Mean annual air temperature is approximately 4°C and mean annual precipitation is approximately ~~1080~~ 1'080 mm (PRISM Climate Group, 2012). On average 80 % of the precipitation falls as snow. Similar to the sites in the ~~Eastern~~ eastern Swiss Alps, two forested sites and one non-forested site were chosen to limit influence of slope and topographic shading while capturing diversity in canopy density and canopy structure.

~~At one forested site, total snow depth~~ At both forested sites, measurements were taken along 20-m forested transects every 0.5 m before and after ~~two storm eventsduring winter 2015/2016 along four parallel 20-m forested transects every~~ storm events. The after storm event transect was parallel to the before storm event transect but displaced by 0.5 m ~~(~~to avoid impacts from the before storm event transect (yellow inlet in Fig. 1b ~~) as well as at a~~ corresponds to each yellow dot). At one non-forested ~~meadow location (open site). At the second forested site , only one snow storm was captured by pre- and post-storm total snow depth measurements along two parallel 20-m transects. Since~~ reference site (open field site) (see blue dots in Fig. 1b) several disordered measurements were conducted within a fenced meadow site (20x20 m^2) (see blue dot in Fig. 1b). Additionally, an automatic weather station nearby provided continuous measurements (Usu Doc Daniel SNOTEL site) (purple dot in Figure 1b). Because the purpose of the Utah measurement campaigns was not to measure snow interception but rather to investigate spatial variability of snow characteristics below different forest canopies (Teich et al., 2019), the derivation of snow interception differed slightly from the Swiss sites. ~~Interception was~~ Accumulated snowfall was first estimated as the difference between pre- and post-storm total snow depth. Then snow interception was calculated by subtracting the total snowfall derived in the forest from the total snowfall derived at the open field site.

During winter 2015/2016 several measurement campaigns took place. We selected those campaigns that allowed to reliably derive snow interception from total snow depth measurements before and after storm events. At one of the forested sites we used four parallel 20-m transects (i.e. two storm events) and at a second forested site two parallel 20-m transects (i.e. one storm event). Every time total snow depth was also measured at the non-forested meadow location (open site). Post-storm measurements were ~~taken~~ made anywhere between approximately ~~one to three~~ 1 to 3 days after a recent snowfall but the total time period between every first and second campaign lasted several days including multiple snowfalls. The storm events were also temporally close, so that ~~all the trees were not~~ trees may not have been snow free prior to new snowfall. As such, unloading and snow settling may have influenced these measurements. After parsing the data to further reduce such influences, 95 individual interception measurements remained, resulting in three site ~~means and three standard deviations to validate parameterizations developed from the Swiss data set~~based mean and standard deviation values. For all individual measurements, a mean snow interception efficiency of 33 % was measured with values ranging from 2 to 93 %. The *pdf* of all individual snow interception data can be similarly well fitted with a normal distribution (positive part) with a RMSE of the

quantiles between both distributions of 1.3 cm and a Pearson correlation r of 0.98 for the quantiles (Fig. 3). Average storm values of air temperatures covered cold (-7.33 °C) to mild (-1.4 °C) conditions.

A ~~1 m^2~~ 1-m resolution gridded LiDAR DSM was generated from a flyover in July of 2009 and encompasses all field ~~areas (Mahat and Tarboton, 2012; Teich and Tarboton, 2016) (~~sites (Mahat and Tarboton, 2012; Teich and Tarboton, 2016) (see Fig. 1b for the extent). The initial point cloud had on average 7 returns/m^2 and 5 last returns/m^2 (shot density). The ~~1 m~~1-m^2 resolution LiDAR DSM is used for the derivation of the canopy structure metrics σ_z and F_{sky} over each 20-m transect (field site).

2.3 Southeastern French Alps

For the second validation data set, indirect interception measurements were collected in a coniferous forest stand next to the mid-altitude experimental site Col de Porte (45.30°N, 5.77°E) at 1325 m a.s.l. in the Chartreuse mountain range in the French Alps (more site details in Morin et al. (2012); Lejeune et al. (2019)). The ~~dominant~~ forest stand is dominated by Norway spruce (*Picea abies*), with young silver fir (*Abies alba*) in the understory. Small deciduous trees are present along the ~~north-west~~ northwest border of the experimental site. Mean annual air temperature is 6°C and the average solid precipitation at Col de Porte is 644 ~~kg/m^2~~ mm per year.

~~New~~ All snow depth measurements were ~~collected in one forested field area during pre- and post-storm events~~ taken by the Snow Research Center (Centre d'Etude de la Neige (CEN)) ~~)~~ in Grenoble, France as part of the Labex SNOUF project (SNow Under Forest) (Vincent et al., 2018) (Fig. 1c)~~next to the Col de Porte experimental site (Vincent et al., 2018)~~. There were three 8-m transects, each consisting of eight ~~1 m~~ 1-m x 0.39~~m~~ -m wooden boxes that were aligned along the ~~North, South and West~~ north, south and west axes of the field ~~area~~site. New snow depth was measured inside each box after a storm event and was then cleared of snow. Open ~~area~~ site new snow depth measurements were obtained from snow board measurements ~~from the Col de Porte~~ at the experimental site. The boards were cleaned after each precipitation event. Interception was then derived as the difference between the open ~~area~~ site and under-canopy new snow box measurements.

During winter 2017/2018 several measurement campaigns were conducted. Four snow storm events were selected after which new snow depth was measured in all boxes. Snow depth was collected after a major storm event took place. Unloading was ~~controlled visually and from webcams . As such, unloading~~ visually observed from webcams and had a minimal influence on the measurements. ~~Four snow storm events during 2018 were selected for a~~ A total of 96 individual interception measurements (4x24 measurements) ~~and~~ resulted in four site ~~means~~ based mean and standard deviation values~~for the second independent validation data set~~. For the individual measurements, a mean snow interception efficiency of 66 % was measured with values ranging from 1 to 94 %. The *pdf* of all snow interception data can be roughly fitted with a normal distribution (positive part) with a RMSE of the quantiles between both distributions of 1.1 cm and a Pearson correlation r of 0.96 for the quantiles (Fig. 3). Average storm values of air temperatures covered mild (-0.9 °C) to warm (1.7 °C) conditions.

A ~~1 m^2~~ 1-m resolution gridded LiDAR DSM was generated from ~~a flyover~~ flyovers between 30 August and 2 September 2016 ~~and encompasses~~ encompassing the entire Col de Porte experimental site (IRSTEA, Grenoble (see Fig. 1c)). The initial LiDAR point cloud had an average density of 24 points /m^2 and a shot density of 17 points/ m^2 (last return). The initial point

cloud right at the transects had an average density of 42 points /m^2 and a shot density of 25 points/ m^2 (last return). The ~~1 m~~1-m^2 resolution LiDAR DSM is used for the derivation of the canopy structure metrics σ_z and F_{sky} over the three 8-m transects.

3 Methods

Subgrid parameterizations were derived for site means and standard deviation of snow interception using forest structure metrics and open ~~area~~ site snowfall. We parameterize mean and spatial variability of snow interception for a model grid cell by accounting for the unresolved underlying forest structure (subgrid parameterization). Forest structure metrics are derived from DSM's to integrate both the terrain elevation and vegetation height.

3.1 Forest structure metrics

The sky view factor F_{sky} describes the proportion of a radiative flux received by an inclined surface patch from the visible part of the sky to that obtained from an unobstructed hemisphere (Helbig et al., 2009). F_{sky} is a commonly applied model parameter when computing surface radiation balances and can be easily computed for large areas from DSM's. F_{sky} integrates previously applied forest structure metrics, such as total open area and mean distance to canopy, ~~since~~ because this parameter is able to account for distance, size and orientation of individual surface (or canopy) patches (Helbig et al., 2009). We therefore selected F_{sky} to parameterize the site mean and standard deviation of snow interception (I_{HS}, σ_{HS}). Here, we compute F_{sky} from view factors which are geometrically derived quantities. They can be computed by numerical methods described within the radiosity approach for the shortwave (SW) radiation balance over complex topography (Helbig et al., 2009) and were originally introduced to describe the radiant energy exchange between surfaces in thermal engineering (Siegel and Howell, 1978). Thereby, Helbig et al. (2009) solve the double area integral using uniform but adaptive area subdivision for surface patches A_I, A_J. F_{sky} for each surface patch A_I is one minus the sum over all N view factors F_{IJ} by assuming the sky as one large surface patch. F_{sky} is computed for each fine-scale grid cell of the DSM:

$$F_{I,\text{sky}} = 1 - \sum_{J=1}^{N} F_{IJ} = 1 - \sum_{J=1}^{N} \frac{1}{A_I} \int_{A_I} \int_{A_J} \frac{\cos\vartheta_I \, \cos\vartheta_J}{\pi \, r_{IJ}^2} \, \mathrm{d}A_I \, \mathrm{d}A_J \, . \tag{1}$$

Deriving F_{sky} via Eq. (1) can account for holes in the surface, i.e. small gaps between leaves and branches in forest canopy, provided the DSM is of a high enough resolution to capture this. In this study, the employed DSM's did not resolve small gaps between branches. Common methods to derive F_{sky} for forested regions is from sine and cosine weighted proportions of sky pixels of HP or SP as suggested e.g. by Essery et al. (2008) or from LAI (e.g. Roesch et al., 2001). However, compared to computing F_{sky} on DSM's these methods rely on extensive field work.

The main advantage in deriving F_{sky} on DSM's is that F_{sky} can be derived spatially by averaging all fine-scale F_{sky} within a coarse grid cell. Here, we use the spatial mean of the sky view factor F_{sky} Eq. (1) over a field site which is comparable to the spatial mean canopy openness.

The second forest structure metric selected was the standard deviation of the DSM σ_z of a field ~~area~~site. Though not totally uncorrelated from the spatial mean F_{sky} (Pearson r=~~-0.41~~-0.48), we selected σ_z to serve in coarse-scale models that are not able to rely on computational expensive pre-computations of F_{sky} on fine scales, such as land surface models covering regions of several hundreds to thousands of kilometers. σ_z is thought to represent the spatial ~~heterogeneity~~ variability of canopy height and terrain elevation of the field site (or model domain).

3.2 Subgrid parameterization for forest canopy interception

~~Parameterizations for~~ Modeling forest canopy involves several processes such as interception, unloading, melt and drip, and sublimation. Here, we present novel models for the spatial mean and standard deviation of snow interception. Modeling not only the mean but the standard deviation of snow interception within a grid cell or model domain opens new possibilities to describe the spatially varying snow cover in large grid cells. Empirical parameterizations for site mean and standard deviation of snow interception ~~were~~ are derived from the 60 measured mean and standard deviation values from the Swiss data set. Estimates derived using the new ~~parameterizations~~ models were validated from a comparison to the mean and standard deviation values from the French and U.S. field sites. ~~However, snow~~

Snow interception I was modeled as snow depth HS, i.e. I_{HS}, and not as snow water equivalent SWE~~to remove~~, i.e. I_{SWE}. Snow interception models for SWE would be advantageous for model applications because this removes uncertainties of the consequent empirical snow density parameterization in each model application. However, at the moment similar spatial SWE interception measurements comparable to the extensive, spatial snow depth interception data set from Switzerland are not available. The reason similar SWE data sets do not exist is probably that SWE measurements require much more effort and are more time-consuming. We further refrained from deriving a spatial SWE data set from the spatial HS interception data set to avoid any potential error ~~when~~ introduced when empirically converting measured HS values to SWE. Thus, any future snow density model developments should not affect our snow interception models. Previous interception models ~~(Hedstrom and Pomeroy, 1998; Schmidt and Gluns, 1991; Moeser et al., 2015b)~~ (Hedstrom and Pomeroy, 1998; Moeser et al., 2015b; Ro estimated new snow density to convert HS into SWE. Models of new snow density typically rely on average storm temperature. ~~This introduces a bias and prior~~ Thus, converting HS empirically to SWE and then developing an empirical interception model introduces additional uncertainty. Prior work has shown a standard error of 9.31 kg/m^{-3} when using estimates of density (Hedstrom and Pomeroy, 1998). As such, the snow interception parameterizations developed here are for HS.

From here on, all references will be to site values (mean and standard deviation) without explicitly mentioning the 'mean', unless otherwise stated.

3.3 Performance measures

We use a variety of measures to validate the parameterizations: the ~~Root-Mean-Square Error (RMSE)~~RMSE, Normalized Root-Mean-Square Error (NRMSE~~) (~~, normalized by the range of data), Mean-Absolute Error (MAE), the Mean Percentage Error (MPE~~) (Bias~~, bias with measured-parameterized normalized with measurements) and the Pearson correlation coefficient r as a measure for correlation. Finally, we evaluate the performance of our parameterizations by analyzing the pdf's. We use the

two-sample Kolmogorov-Smirnov test (K-S test) statistic values D (Yakir, 2013) for the *pdf*'s (nonparametric method) and compute the NRMSE for Quantile-Quantile plots ($\text{NRMSE}_{\text{quant}}$) for probabilities with values in $[0.1, 0.9]$.

4 Results

4.1 Grid cell mean snow interception

4.1.1 ~~Parameterization~~Model for grid cell mean intercepted snow depth

We parameterized grid cell mean intercepted snow depth (I_{HS}) by scaling open ~~area~~ site accumulated snowfall P_{HS} using the forest structure metrics F_{sky} and σ_z. From these three variables, the interception measurements of the development data set correlated best with P_{HS} ($r = 0.70$). Snow interception efficiency (I_{HS}/P_{HS}) correlations were slightly stronger for σ_z ($r = 0.71$) than for F_{sky} ($r =$ ~~-0.63~~-0.69).

Based on ~~observed relationships and~~ the previously presented relationships and observed correlations we developed two statistical parameterizations for I_{HS} using two different base functions to scale P_{HS} with either F_{sky} and σ_z (Eq. (2)) or with only σ_z (Eq. (3):

$$I_{HS} = P_{HS}^{\text{a}} \frac{(1 - F_{\text{sky}}^{\text{b}})\,\sigma_z^{\text{c}}}{1 + exp(-\text{d}\,(P_{HS} - \text{f}))} \text{b} \frac{(1 - F_{\text{sky}})^{\text{c}}\,\sigma_z^{\text{c}}}{1 + exp(-\text{d}\,(P_{HS} - \text{f}))} \tag{2}$$

with constant parameters: a~~= 0.6417, b= 1.0868, c= 0.7063, d= 0.1597 and f= 6.6884~~ = 0.09 (±*1.08*), b= 0.19 (±*0.79*), c= 0.72 (±*0.11*), d= 0.13 (±*0.04*) and f= 16.44 (±*16.33*) and

$$I_{HS} = P_{HS}^{\text{a}^\star}\,\text{b}^\star\,\sigma_z^{\text{c}^\star} \tag{3}$$

with constant parameters: a~~* = 0.8199, b* = 0.1424 and c* = 0.8002~~* = 0.82 (±*0.12*), b* = 0.0035 (±*0.0036*) and c* = 0.80 (±*0.14*). The constant parameters ~~resulted~~ result from fitting non-linear regression models by robust M-estimators using iterated reweighed least squares (see R v3.2.3 statistical programming language robustbase v0.92-5 package (Rousseeuw et al., 2015)). The 90 % confidence intervals of the parameters are given in parentheses. In both equations P_{HS} and σ_z are in cm.

The accuracy of a derived model between I_{HS} and P_{HS} depended upon the forest structure metrics and the underlying function applied in the potential models. ~~The~~ While we investigated previously suggested functional dependencies for the amount of storm snowfall the best performances were seen when the base function between I_{HS} and P_{HS} was either a power law or a combination of a power law with an exponential dependence~~similar to the one suggested by Moeser et al. (2015b)~~. Similar base functions were obtained for fine-scale I_{SWE} models by Moeser et al. (2015b) (exponential) and recently by Roth and Nolin (2019) (power law).

Estimated I_{HS}-values from Eq. (2) or (3) increase with increasing P_{HS}, increasing σ_z or decreasing F_{sky}. This implies that with ~~decreasing~~ increasing forest density (i.e. ~~more canopy surface is exposed~~larger σ_z), I_{HS} increases faster with increasing P_{HS}. Note that here, a lower F_{sky} value denotes more pronounced forest gaps since it is derived from aerial LiDAR DSM~~in contrast to ground based *HP* acquired below canopy. where this relationship is reversed.~~ .

Eq. (2) and (3) differ in two ways. First, Eq. (2) incorporates the functional dependency for increasing P_{HS} that snow interception efficiency (interception/snowfall) increases with increasing precipitation due to snow bridging between branches until a maximum is reached after ~~that~~ which it decreases due to bending of branches under the load (sigmoid curve as suggested by ~~Moeser et al. (2015b)~~Satterlund and Haupt (1967); Moeser et al. (2015b)). Additionally, a power law dependency for accumulated open ~~area~~ site storm snowfall is applied to force the sigmoid distribution to zero at very small snowfall events. The sigmoid curve alone is not able to reach zero, potentially breaking the mass balance. In contrast, Eq. (3) solely employs the power law dependency between I_{HS} and accumulated open ~~area~~ site storm snowfall P_{HS}. The second difference between both equations is that Eq. (2) uses both forest structure metrics (F_{sky} and σ_z), whereas Eq. (3) only uses σ_z. Eq. (2) is thus more 'complex~~,~~'', and necessitates more time to derive both forest structure parameters whereas Eq. (3) has a more 'compact' form and solely necessitates estimation of σ_z.

4.1.2 Validation of model for grid cell mean intercepted snow depth

Performances of both newly developed snow interception I_{HS} models (Eq. (2) and (3)) were compared to the I_{HS} measurements from the development data set (Switzerland), as well as the I_{HS} measurements from the combined two geographically and ~~climatological~~ climatologically different validation data sets (France and ~~United States~~U.S.). In ~~Fig. s~~ Figs. 4 to 6 we differentiate the validation data set from the development data set by using a black outline around the symbols (validation) instead of colored circles (development). Squares represent the data set from the U.S. and diamonds represent the data set from France.

Fig. 4 displays that, for both models, there is a good agreement for I_{HS} to measured interception at all sites. Overall error statistics show good performances for the development and the validation data sets with low absolute errors (e.g. all MAE$\leq$1.2 cm), strong correlations (all $r \geq$~~0.9~~0.89) and low distribution errors (e.g. all $\text{NRMSE}_{\text{quant}}$~~lower 10~~ <8 %) (Table 1). In contrast to the validation data ~~set,s~~ sets performance statistics for the development data set are slightly reduced for the more compact model (Eq. (3)) compared to the more complex model (Eq. (2)).

Fig. 5 reveals overall similar performances for both parameterizations as a function of accumulated ~~snow fall~~new snowfall. However, small differences between both parameterizations are visible in the extremes, i.e. for very low and very large I_{HS} and P_{HS}. The bias for the largest P_{HS} (U.S. data set) is ~~slightly~~ larger for the more ~~complex~~ compact parameterization (Eq. (~~2~~3)) whereas for the smallest P_{HS} (data set from France) the bias is slightly larger for the more ~~compact~~ complex parameterization (Eq. (~~3~~2)). The bias is more pronounced with regard to the corresponding interception efficiencies, shown in Fig. 5d-f, the largest bias for the smallest P_{HS} for the ~~compact~~ complex parameterization (Eq. (~~3~~2)) is ~~-0.23 compared to 0.09~~ -0.24 compared to 0.21 for the more ~~complex~~ compact parameterization (Eq. (~~2~~3)).

4.2 Grid cell standard deviation of snow interception

4.2.1 ~~Parameterization~~Model for standard deviation of snow depth interception

We parameterized the standard deviation of snow depth interception $\sigma_{I_{HS}}$ by scaling P_{HS} using the forest structure metric σ_z. $\sigma_{I_{HS}}$ of the development data set correlated best with P_{HS} ($r = 0.82$). The correlation with mean snow interception I_{HS} was less pronounced ($r = 0.33$). $\sigma_{I_{HS}}$ normalized with P_{HS} correlated much better with σ_z (r = -0.68) than with F_{sky} (r = ~~0.1~~0.13).

Building upon the observed power law functional dependency between mean snow interception I_{HS} and P_{HS} and the observed relationships and correlations for $\sigma_{I_{HS}}$ we scaled a power law function for P_{HS} with the standard deviation of the DSM σ_z in order to parameterize $\sigma_{I_{HS}}$:

$$\sigma_{I_{HS}} = P_{HS}^{\text{g}} \underline{\text{h}\,\sigma_z^{\text{j}}} \frac{\text{h}}{1+\sigma_z^{\text{j}}} \,. \tag{4}$$

Constant parameters g~~= 0.7821, h= 1.0826 and j= −0.5175~~ = 0.78 (±*0.10*), h= 13.40 (±*11.64*) and j= 0.53 (±*0.12*) result from fitting a non-linear regression model, similar to the derivation of I_{HS} from Eq. (2) and (3). The 90 % confidence intervals of the parameters are given in parentheses. In Eq. (4) P_{HS} and σ_z are in cm.

$\sigma_{I_{HS}}$ derived from Eq. (4) increases with increasing P_{HS} or decreasing σ_z. This implies that ~~as canopy height becomes more homogeneous~~with decreasing σ_z (decreasing forest density), the spatial variability in snow interception increases faster with increasing P_{HS}. The opposite correlation was found between σ_z and mean snow interception I_{HS}. For a σ_z converging to zero, modeled $\sigma_{I_{HS}}$ via Eq. (4) approaches a constant fraction of precipitation.

4.2.2 Validation of model for standard deviation of snow depth interception

Overall, modeled and measured $\sigma_{I_{HS}}$ agree well (Fig. 6). Error statistics show good performances for the development and the validation data set with low absolute errors (e.g. all MAE≤~~0.64~~ 0.63 cm), strong correlations (all $r \geq$0.92) and low distribution errors (e.g. $\text{NRMSE}_{\text{quant}}$ ~~lower~~ <10 %) (Table 1). However, performances are less accurate for the validation data set than for the development data set (e.g. MAE of ~~0.64~~ 0.63 cm as opposed to 0.45 cm and $\text{NRMSE}_{\text{quant}}$ of 10 % as opposed to 4 %). This was caused by a potential outlier in the validation data set from the U.S. ~~.~~ During one measurement campaign, an open ~~area~~ site accumulated storm snowfall P_{HS} was not available at the same date as the under canopy measurements. Therefore, this value was estimated from a local automatic weather station (Usu Doc Daniel SNOTEL site; purple dot in Figure 1b). Additional measurement uncertainty (at the Utah site) was also introduced, since interception estimates were integrated values over several snow storms that occurred during the 13 days between pre- and post- ~~snow fall~~ snowfall measurement campaigns. When this outlier is removed from the validation data set, performance statistics improve considerably converging towards the errors of the development data set, cf. MAE decreases to 0.35 cm and the $\text{NRMSE}_{\text{quant}}$ to 5 %.

To compare modeled ~~and~~ (Eq. (2) and Eq. (4)) and measured data set mean values from each geographic location (Switzerland, ~~US~~U.S., France), we averaged all site values to derive an overall mean of I_{HS}, and $\sigma_{I_{HS}}$ for each location. The coefficient

of variation (description of variability) ($CV_{I_{HS}}$=$\sigma_{I_{HS}}/I_{HS}$) was also calculated for each of the three geographic locations. For the Swiss development data set, the same overall mean~~and standard deviation~~ , standard deviation and CV for measured and modeled snow interception was calculated (mean of ~~4.5 cmand~~ 9.4 cm, standard deviation of ~~9.4 cm), and the~~ 4.5 cm and CV ~~was almost equivalent (~~of 0.51~~versus 0.50~~). For the validation data sets we obtained slightly larger values for modeled I_{HS} (~~9.4~~ 9.3 cm), modeled $\sigma_{I_{HS}}$ (3.7 cm) and modeled $CV_{I_{HS}}$ (~~0.40~~0.38) than measured I_{HS} (9.2 cm), measured $\sigma_{I_{HS}}$ (3.2 cm) and measured $CV_{I_{HS}}$ (0.35). If the potential outlying data point from Utah is removed, the same overall modeled and measured mean $CV_{I_{HS}}$ (~~0.31~~0.32) is found along with very close values of modeled and measured mean I_{HS} (~~10.1~~ 9.8 cm versus 9.9 cm) and modeled and measured $\sigma_{I_{HS}}$ values (3.4 cm versus 3.3 cm).

5 Discussion

We proposed two empirical models for spatial mean interception I_{HS} to be employed in hydrological, climate and weather applications. One model is a more compact model, Eq. (3). This model uses a power law dependency between I_{HS} and accumulated storm precipitation P_{HS} that is scaled by one forest structure metric: the standard deviation of the DSM σ_z. The other model, Eq. (2), integrates a more complex parameterization by using a combination of a power law with an exponential dependence similar to the one suggested by Moeser et al. (2015b) for P_{HS} and is scaled by two forest metrics: the sky view factor F_{sky} in combination with σ_z. For both I_{HS} models, interception increases faster with increasing snowfall when forest density ~~decreases~~ increases (i.e. ~~more canopy is exposed~~larger σ_z). In the more complex model ~~decreasing~~ increasing forest density is implemented by increasing σ_z and decreasing F_{sky}. Though F_{sky} can be pre-computed and is temporally valid for many years (unless the forest structure changes due to logging, fires, insect infestations or other forest disturbances), computing F_{sky} over large scales and/or with fine resolutions is more computationally demanding than for σ_z (Helbig et al., 2009). A subgrid parameterization for the sky view factor of coarse-scale DSM's over forest canopy would eliminate the pre-computation of sky view factors on fine-scale DSM's. Such a subgrid parameterization for sky view factors over forest canopy could be similarly set up as previously done for alpine topography and would lead us towards a global map of sky view factors (cf. Helbig and Löwe, 2014).

In general, more differences between the compact and more complex modeling approaches only displayed at the extremes. For instance, for small storm precipitation values (P_{HS} =3 cm), the more ~~complex parameterization performs~~ compact parameterization performs slightly better whereas for very large storms (P_{HS} =43 cm), the more ~~compact~~ complex model displayed improved performance. The choice ~~for~~ of one of these two models thus depends on ~~field area characteristics, desired accuracy~~ the focus range of precipitation values and available computational ~~cost and storage.~~ resources.

Our choice for the functional form of P_{HS} differs from previous parameterizations for snow interception solely using the sigmoid growth $\sim 1/(1+exp(-k(P-P_0)))$ (e.g. Satterlund and Haupt, 1967; Schmidt and Gluns, 1991; Moeser et al., 2015b) or an exponential form $\sim (1-exp(-k(P-P_0)))$ (e.g. Aston, 1993; Hedstrom and Pomeroy, 1998) with increasing precipitation. While the base function of Satterlund and Haupt (1967) worked better for Moeser et al. (2015b), a drawback of this relationship is that interception does not become exactly zero for a zero snowfall amount. To account for this, the model becomes complicated

when applied to discrete model time steps (Moeser et al., 2016). For this reason, Mahat and Tarboton (2014) selected the relationship proposed by Hedstrom and Pomeroy (1998) for their parameterization of snow interception. However, the functional form of the Hedstrom and Pomeroy (1998) model does not account for snow bridging or branch bending, thus modeling interception efficiency as decreasing through time. We also compared means and standard deviations over all sites as a function of forest metrics and found that the use of storm means can introduce precipitation dependencies that might originate from an insufficient number of sites showing similar forest canopy structure parameter values for a given precipitation (cf. black line compared to colored dots in Fig. (5)). Based on the functional dependencies revealed by analyzing our data as a function of P_{HS} and forest structure metrics, a simple power law was able to describe the spatial mean P_{HS} dependency of snow interception (cf. Eq. (3)). The equation displayed that with increasing P_{HS}, I_{HS} increases. This is less pronounced with smaller σ_z or larger F_{sky} values (Fig. (5)). Very recently, a storm event power law dependency was also found to best describe fine-scale SWE interception in a maritime snow climate (Roth and Nolin, 2019). Our base functions for site means and standard deviations thus bear some similarity to previously developed fine-scale snow interception models. Despite an ongoing debate regarding the proper representation of interception, we believe that the interception models presented here have the advantage that they could be applied in various model applications for horizontal grid cell resolutions larger than a few tenth of meters. Due to the lack of measurements over larger scales a validation remains however at the moment impossible.

We have derived just one empirical model for the standard deviation of snow interception $\sigma_{I_{HS}}$ that uses a power law dependency on accumulated storm precipitation P_{HS} scaled by one forest structure metric: the standard deviation of the DSM σ_z. We also tested a more complex model for $\sigma_{I_{HS}}$ using both forest metrics (F_{sky} and σ_z) that also integrates a power law dependency of P_{HS}. However, model performances for the validation data set did not differ considerably from the ones for the more compact model. Therefore, we propose the more compact parameterization for $\sigma_{I_{HS}}$ (Eq. (4)) to facilitate broad model applications.

By using F_{sky} and σ_z derived from DSM's as forest structure metrics we focused on the overall shape of the forest. This simplification is similar to the assumption by Sicart et al. (2004) for solar transmissivity in forests under cloudless sky conditions. They assumed the fraction of solar radiation blocked by the canopy was equal to 1-Vf_f with V_f therein being defined as the fraction of the sky visible from beneath the canopy. Our simplification is also in line with previous suggestions. Primarily, to reliably describe interception by forest canopy over larger areas, the larger-scale canopy structure needs to be taken into account instead of only using point based canopy structure parameters (e.g. Varhola et al., 2010; Moeser et al., 2016). We proposed to calculate F_{sky} and σ_z on DSM's rather than on CHM's to account for terrain and vegetation height. This results from our correlation analysis for measurement data collected in rather flat field forest sites (Section 2) and should be verified once spatial snow interception measurements become available in steeper terrain and over larger length scales.

The models for I_{HS} and $\sigma_{I_{HS}}$ were statistically derived from measured snow interception data gathered in the ~~Eastern~~ eastern Swiss Alps. ~~We displayed~~ Naturally, empirically derived parameterizations can only describe data variability covered by the data set. However, even though the parameterizations were developed empirically, we could display that the parameterizations perform well for two disparate, independent snow interception data sets collected in geographically different regions, different snow climates, coniferous tree species and prevailing weather conditions during collection of the validation data

sets (French Alps and Rocky Mountains, U.S.). For instance, in the French Alps, rather warm to mild winter weather conditions predominated whereas rather mild to cold weather prevailed during the campaigns in the Rocky Mountains of ~~Northern~~ northern Utah in the U.S. ~~.~~ Though snow cohesion and adhesion are clearly temperature dependent, we did not observe decreases in overall performances under these differing weather conditions for our two I_{HS} models, which do not include air temperature. In contrast, in a maritime (warm) snow climate correlations between air temperature and snow interception were recently found ~~Roth and Nolin (2019). Our ranges of interception and~~ by Roth and Nolin (2019). In addition to the spread in observed temperature conditions, our ranges of accumulated snow storm P_{HS} values of the development data set are fairly broad (e.g. P_{HS} between 10 cm and 40 cm). The measurements of the validation data set are well within the range of the development data set values, ~~with the exception of~~ but also cover extremes, such as one very small (P_{HS}= 3 cm) and one very large ~~snow fall~~ snowfall (P_{HS}= 43 cm) (cf. Fig. 3). ~~Given the large development data set(Moeser et al., 2015b) and the~~ It is thus reassuring that our models, perform sufficiently well in varying climate regions though clearly more validation data sets would be advantageous especially in regions experiencing extreme climates such as the cold arctic or warm maritime forests. Despite the existing variability in the data set, more spatial snow interception measurements would clearly help to increase the robustness of our empirical parameterizations. However, with the overall good performance of the parameterizations for the validation data ~~set, it is reassuring that our models, perform sufficiently well in varying climate regions. This lends~~ sets and the development data set of Moeser et al. (2015b) currently being probably the most extensive existing data set for spatial snow interception, our results lend validity to the models for a range of coarse-scale model applications such as in climate, hydrologic (watershed and snow), and meteorological models.

Despite the overall good performance of the models, we observed differences between the two validation data sets. The data set collected in France shows improved error statistics for snow interception I_{HS} (e.g. for Eq. (3): RMSE=0.35 cm, NRMSE=4 %, MAE=~~0.28 cm, r= 1 and NRMSE$_{quant}$= 3 %~~0.26 cm) as compared to the data set collected in the U.S. (e.g. for Eq. (3): RMSE=1.52 cm, NRMSE=14 %, MAE=~~1.5 cm, r= 0.95 and NRMSE$_{quant}$= 12 %~~1.4 cm). In France, intercepted snow storm depth was measured as the difference of new snow depth in wooden boxes below trees and open ~~area~~ site new snow storm depth. This was done in relatively short time intervals after a snow storm. In the U.S., intercepted snow was inferred from ~~absolute snow depth differences~~ total snow depth before and after a snow storm event within forests and in an open ~~area~~site. Derived snow interception was often integrated over several storm events due to longer periods between the measurement campaigns. Thus, these measurements were ~~influenced by~~ potentially influenced by other snow and forest processes such as snow settling, wind redistribution, sublimation, unloading~~and melt~~, and melt and drip. Our interception models ~~do not account for such effects. We~~ however only calculate how much snow is intercepted at any point in time, which provides the input for other forest snow process models such as for unloading, sublimation as well as melt and drip. We thus assume that these processes will be addressed separately, as in all prior interception models (Roesch et al., 2001). ~~Our approach also does not define a maximum interception capacity, i.e. the maximum possible load on forest canopy (e.g. Schmidt and Gluns, 1991; Hedstrom and Pomeroy, 1998; Roesch et al., 2001; Essery, 2013; Moeser et al., 2015a).Another reason for the differences in model performances could~~ Despite some uncertainties in the validation data set from the U.S. it

allowed for validation in a different snow climate than the French Alps and also covered a large spread in storm snowfall amounts (Fig. 4).

Differences in model performances between the two validation data sets could also be attributed to the more accurate forest structure metrics for the French data set because of a higher resolution LiDAR DSM (higher point density of 24 /m^2 returns and 17 /m^2 last returns) compared to the LiDAR flyover from the U.S. (on average 7 returns/m^2 and 5 last returns/m^2). ~~Despite some uncertainties in the validation data set from the U. S. it allowed for validation in a different snow climate than the French Alps and also covered a large spread in storm snowfall amounts (Fig. 4).~~ While it is clear that the higher the point cloud density, the greater the potential detail of derived DSM's, 1-m resolution DSM's computed from point clouds above 5 returns/m^2 are usually quite consistent, and are suitable to derive coniferous canopy models allowing tree-level analyses (Kaartinen et al., 2012; Eysn et al., 2015). Current available or scheduled country-wide data sets are now around 1-5 returns/m^2 (e.g. Federal Office of Topography Swisstopo, last access: 22 November 2019; Danish Geodata Agency, last access: 22 November 2019; I and these densities can be expected to increase thanks to technical improvements in LiDAR sensors. Since fine-scale DSM's are the only input required to derive the forest structure metrics F_{sky} and σ_z a global applicability of our snow interception models for coniferous forest would be possible with minimal required information.

To understand if the models would also work in other forest types or in disturbed forests, e.g. due to logging, fires or insect infestations, more snow interception measurements in ~~different,~~ deciduous and mixed as well as ~~in~~ disturbed forests are required. Very recently Huerta et al. (2019) showed that previously published snow interception models developed for coniferous forests from Hedstrom and Pomeroy (1998); Lundberg et al. (2004); Moeser et al. (2016) required recalibration to match observed point snow interception observations in a deciduous southern beech *Nothofagus* stand of the ~~Southern~~ southern Andes. We ~~also investigated the model performance~~ investigated the performance of our models for two measurement campaigns in a deciduous quaking aspen (*Populous tremuloides*) forest in our U.S. field site. The measurement setup (20-m transects) was identical to the ones in the coniferous forest at this location (see Section 2.2). Though overall the models compared well with the measurements, the model performance was not as good as for the coniferous forest. ~~Since~~ Because the LiDAR DSM was acquired in the summer, i.e. with leaves on the trees, the models naturally overestimated I_{HS} and $\sigma_{I_{HS}}$. For instance, using the more complex model for I_{HS} (Eq. (2)) we obtained a mean bias of ~~-5.6 cm, respectively~~ -6 cm, whereas when using the more compact model for I_{HS} (Eq. (3)) we obtained a mean bias of ~~-8.2~~ -8 cm. For $\sigma_{I_{HS}}$, the performance was overall slightly better with a mean bias of ~~-3.2~~ -3 cm (Eq. (4)). While this shows that the performance is clearly lower in such sites, we assume that the performance would be improved when the LiDAR is acquired in leaf-off conditions.

The ~~LiDAR-derived~~ LiDAR-derived DSM sky view factors do not account for small spaces between leaves or branches, which are well accounted for when sky view factors are derived from HP or LAI. In principle, sky view factors that are computed on DSM's represent, depending on the return signal used to create the DSM, a coarser view on the underlying forest canopy. While this increases ~~fine scale~~ the overall fine-scale error, we feel that the ability to calculate both our canopy structure metrics in the Cartesian DSM space~~far outweighs fine scale~~, which allows an easy model application, far outweighs fine-scale resolution losses.

~~Our choice for the functional form of P_{HS} differs from previous parameterizations for interception solely using the sigmoid growth $\sim 1/(1+exp(-k(P-P_0)))$ (e.g. Satterlund and Haupt, 1967; Schmidt and Gluns, 1991; Moeser et al., 2015b) or an exponential form $\sim (1-exp(-k(P-P_0)))$ (e.g. Aston, 1993; Hedstrom and Pomeroy, 1998) with increasing precipitation and P_0 as the accumulated storm snow depth at the time of maximum interception efficiency. While the functional form of Satterlund and Haupt (1967) worked better for Moeser et al. (2015b), a drawback of this relationship is that interception does not become exactly zero for a zero snowfall amount. To account for this, the model becomes complicated when applied to discrete model time steps (Moeser et al., 2016). For this reason, Mahat and Tarboton (2014) selected the relationship proposed by Hedstrom and Pomeroy (1998) for their parameterization of snow interception. However, this model does not account for snow bridging or branch bending, thus modeling interception efficiency as a decrease through time. We also compared site means and standard deviations as a function of forest metrics and found that the use of storm means can introduce precipitation dependencies which might originate from an insufficient number of sites showing similar forest canopy structure parameter values for a given precipitation (cf. black line compared to colored dots in Fig. (5)). Based on the functional dependencies revealed by analyzing our data as a function of P_{HS} and forest structure metrics, a simple power law was able to describe the P_{HS} dependency of snow interception (cf. Eq. (3)). The equation displayed that with increasing P_{HS}, I_{HS} increases. This is less pronounced with smaller σ_z or larger F_{sky} values (Fig. (5)). Despite an ongoing debate regarding the proper representation of interception, we believe that the interception models presented here can be applied in various model applications for larger spatial scales.~~

6 Conclusion and Outlook

The statistical models for spatial mean and standard deviation of snow interception presented here are a first step towards a more robust consideration of snow interception for various coarse-scale model applications. They were built upon a very large dataset and validated by two other datasets from different geographic regions and snow climates, and performed well for all three sites and under differing weather conditions. For spatial mean interception all NRMSE's were $\leq$10 % and for the standard deviation of interception all NRMSE's were $\leq$13 %.

In our observed snow interception datasets, as much as 68 % and on average 43 % of the cumulative snowfall was retained by coniferous forests (interception efficiency of site means) and as much as 14 % and on average 11 % of the cumulative snowfall was retained by deciduous forests. ~~Thus, these~~ These values compare well to previously observed snow interception in coniferous trees reaching up to 60 % of cumulative snowfall (Pomeroy and Schmidt, 1993; Pomeroy et al., 1998; Storck and Lettenmaier, 2002) and to 24 % of total annual snowfall in a deciduous forest in the ~~Southern Andes~~ southern Andes (Huerta et al., 2019).

The empirical models integrate forest parameters that can be derived from fine-scale DSM's, which can be pre-generated and stored for large regions. One of the presented interception models only relies on the standard deviation of the fine-scale DSM, which is a very efficient way to integrate snow interception in coarse-scale models such as land surface models. This could greatly improve current forest albedo estimates and the subsequent surface energy balance for various model applications such as hydrological, weather and climate predictions.

However, the presented parameterizations were developed and validated for spatial means and standard deviations over horizontal length scales of a few tens of meters. We can only hypothesize that the parameterizations are also valid at coarser length scales due to the use of non-local forest structure parameters~~provided~~ . Representative non-local forest structure parameters require that a DSM of high enough resolution is available to represent subgrid variability of forest structure in the coarse-scale model grid cell. However, there was and probably is, ~~to-date~~to date, no validation data available at large spatial scales. The investigated length scale matches current satellite resolutions (e.g. Sentinel and Landsat), which opens further cross-validation and deployment opportunities with satellite-derived parameters such as surface albedos and fractional-snow covered area. With parameterizations for both ~~,~~ the mean and standard deviation of snow interception by forest canopy, the distribution of intercepted snow depth in forests can now be derived whenever a sufficiently high-resolution DSM is available.

Competing interests. The authors declare that they have no conflict of interest.

Acknowledgements. We thank E. Thibert and É. Mermin, who performed GPS and tree measurements of the site setup at Col De Porte, and J.A. Lutz, S. Jones, J. Carlisle and D.G. Tarboton for their support and the possibility to work at TWDEF. N. Helbig was partly funded by the Federal Office of the Environment FOEN. M. Teich was partly funded by the Swiss National Science Foundation (P2EZP2_155606, P300P2_171236), the Utah Agricultural Experiment Station (UAES), and the USU Department of Wildland Resources. The Labex SNOUF project has been supported by a grant from Labex OSUG2020-ANR10 LABX56. The TWDEF LiDAR data processing was supported by NSF EPSCoR cooperative agreement IIA 1208732 awarded to Utah State University, as part of the State of Utah Research Infrastructure Improvement Award. Any opinions, findings, and conclusions or recommendations expressed are those of the author(s) and do not necessarily reflect the views of the National Science Foundation.

References

Andreadis, K. M., Storck, P., and Lettenmaier, D. P.: Modeling snow accumulation and ablation processes in forested environments, Water Resour. Res., 45, https://doi.org/10.1029/2008WR007042, 2009.

Aston, A. R.: Rainfall interception by eight small trees, J. Hydrol., 42, 383–396, 1993.

Bartlett, P. A. and Verseghy, D. L.: Modified treatment of intercepted snow improves the simulated forest albedo in the Canadian Land Surface Scheme, Hydrol. Process., 29, 3208–3226, https://doi.org/10.1002/hyp.10431, http://dx.doi.org/10.1002/hyp.10431, 2015.

Bründl, M., Bartelt, P., Schneebeli, M., and Flühler, H.: Measuring branch deflection of spruce branches caused by intercepted snow load, Hydrol. Process., 13, 2357–2369, 1999.

Danish Geodata Agency: https://download.kortforsyningen.dk/content/dhmpunktsky, last access: 22 November 2019.

Dirmeyer, P. A., Gao, X., Zhao, M., Guo, Z., Oki, T., and Hanasaki, N.: GSWP-2: Multimodel analysis and implications for our perception of the land surface, B. Am. Meteorol. Soc., 87, 1381–1398, 2006.

Essery, R.: Large-scale simulations of snow albedo masking by forests, Geophys. Res. Lett., 40, 5521–5525, https://doi.org/10.1002/grl.51008, 2013.

Essery, R., Rutter, N., Pomeroy, J., Baxter, R., Stähli, M., Gustafsson, D., Barr, A., Bartlett, P., and Elder, K.: SNOWMIP2: An evaluation of forest snow process simulations, Bull. Am. Meteorol. Soc., 90, 1120–1136, 2009.

Essery, R. L., Pomeroy, J. W., Parviainen, J., and Storck, P.: Sublimation of snow from coniferous forests in a climate model, J. Climate, 16, 1855–1864, 2003.

Essery, R. L., Bunting, P., Hardy, J., Link, T., Marks, D., Melloh, R., Pomeroy, J., Rowlands, A., and Rutter, N.: Scaling and parametrization of clear-sky solar radiation over complex topography, J. Hydrometeorol., 9, 228–241, 2008.

Eysn, L., Hollaus, M., Lindberg, E., Berger, F., Monnet, J.-M., Dalponte, M., Kobal, M., Pellegrini, M., Lingua, E., Mongus, D., and Pfeifer, N.: A Benchmark of Lidar-Based Single Tree Detection Methods Using Heterogeneous Forest Data from the Alpine Space, Forests, 6, 1721–1747, 2015.

Federal Office of Topography Swisstopo: https://www.swisstopo.admin.ch/en/knowledge-facts/geoinformation/lidar-data.html, last access: 22 November 2019.

Hall, A.: The role of surface albedo feedback in climate, J. Clim., 17, 1550–1568, 2004.

Hedstrom, N. R. and Pomeroy, J. W.: Measurements and modelling of snow interception in the boreal forest, Hydrol. Process., 12, 1611–1625, 1998.

Helbig, N. and Löwe, H.: Parameterization of the spatially averaged sky view factor in complex topography, J. Geophys. Res., 119, 4616–4625, https://doi.org/10.1002/2013JD020892, 2014.

Helbig, N., Löwe, H., and Lehning, M.: Radiosity approach for the surface radiation balance in complex terrain, J. Atmos. Sci., 66, 2900–2912, https://doi.org/10.1175/2009JAS2940.1, 2009.

Hellström, R. A.: Forest cover algorithms for estimating meteorological forcing in a numerical snow model, Hydrol. Process., 14, 3239–3256, 2000.

Huerta, M. L., Molotch, N. P., and McPhee, J.: Snowfall interception in a deciduous Nothofagus forest and implications for spatial snowpack distribution, Hydrol. Process., 1-17, https://doi.org/10.1002/hyp.13439, 2019.

Kaartinen, H., Hyyppä, J., Yu, X., Vastaranta, M., Hyyppä, H., Kukko, A., Holopainen, M., Heipke, C., Hirschmugl, M., Morsdorf, F., Næsset, E., Pitkänen, J., Popescu, S., Solberg, S., Wolf, B. M., and Wu, J. C.: An International Comparison of Individual Tree Detection and Extraction Using Airborne Laser Scanning, Remote Sens., 4, 950–974, https://doi.org/10.1016/j.jhydrol.2009.09.021, 2012.

Knowles, N., Dettinger, M. D., and Cayan, D. R.: Trends in snowfall versus rainfall in the western United States, J. Climate, 19, 4545—-4559, 2006.

Krinner, G., Derksen, C., Essery, R., Flanner, M., Hagemann, S., Clark, M., Hall, A., Rott, H., Brutel-Vuilmet, C., Kim, H., et al.: ESM-SnowMIP: assessing snow models and quantifying snow-related climate feedbacks, Geosc. Model Dev., 11, 5027–5049, 2018.

Latvian Geospatial Information Agency: https://www.lgia.gov.lv/lv/Digit%C4%81lais%20virsmas%20modelis, last access: 22 November 2019.

Lejeune, Y., Dumont, M., Panel, J.-M., Lafaysse, M., Lapalus, P., Le Gac, E., Lesaffre, B., and Morin, S.: 57 years (1960–2017) of snow and meteorological observations from a mid-altitude mountain site (Col de Porte, France, 1325 m of altitude), Earth Syst. Sci. Data, 11, 71–88, https://doi.org/10.5194/essd-11-71-2019, https://www.earth-syst-sci-data.net/11/71/2019/, 2019.

Lundberg, A., Nakai, Y., Thunehed, H., and Halldin, S.: Snow accumulation in forests from ground and remote-sensing data, Hydrol. Process., 18, 1941–1955, https://doi.org/10.1002/hyp.1459, 2004.

Mahat, V. and Tarboton, D. G.: Canopy radiation transmission for an energy balance snowmelt model, Water Resour. Res., 48, 1–16, https://doi.org/10.1029/2011WR010438, 2012.

Mahat, V. and Tarboton, D. G.: Representation of canopy snow interception, unloading and melt in a parsimonious snowmelt model, Hydrol. Process., 28, 6320–6336, https://doi.org/10.1002/hyp.10116, 2014.

Moeser, D., Roubinek, J., Schleppi, P., Morsdorf, F., and Jonas, T.: Canopy closure, LAI and radiation transfer from airborne LiDAR synthetic images, Agric. For. Meteorol., 197, 158–168, 2014.

Moeser, D., Morsdorf, F., and Jonas, T.: Novel forest structure metrics from airborne LiDAR data for improved snow interception estimation, Agric. For. Meteorol., 208, 40–49, 2015a.

Moeser, D., Staehli, M., and Jonas, T.: Improved snow interception modeling using canopy parameters derived from airborne LiDAR data, Water Resour. Res., 51, 5041–5059, https://doi.org/10.1002/2014WR016724, 2015b.

Moeser, D., Mazotti, G., Helbig, N., and Jonas, T.: Representing spatial variability of forest snow: Implementation of a new interception model, Water Resour. Res., 52, 5041–5059, https://doi.org/10.1002/2015WR017961, 2016.

Morin, S., Lejeune, Y., Lesaffre, B., Panel, J. M., Poncet, D., David, P., and Sudul, M.: An 18-yr long (1993-2011) snow and meteorological dataset from a mid-altitude mountain site (Col de Porte, France, 1325 m alt.) for driving and evaluating snowpack models, Earth Syst. Sci. Data, 4, 13–21, https://doi.org/10.5194/essd-4-13-2012, 2012.

Morsdorf, F., Kötz, B., Meier, E., Itten, K. I., and Allgöwer, B.: Estimation of LAI and fractional cover from small footprint airborne laser scanning data based on gap fraction, Remote Sens. Environ., 104, 50–61, 2006.

Pomeroy, J. W. and Schmidt, R. A.: The use of fractal geometry in modelling intercepted snow accumulation and sublimation, in: Proc. Eastern Snow Conference, vol. 50, pp. 1–10, 1993.

Pomeroy, J. W., Parviainen, J., Hedstrom, N., and Gray, D. M.: Coupled modelling of forest snow interception and sublimation, Hydrol. Process., 12, 2317–2337, 1998.

PRISM Climate Group: 30-Year Normals, Oregon State University, http://www.prism.oregonstate.edu/normals/ (created 07 November 2012); accessed 28 June 2019, 2012.

Roesch, A. and Roeckner, E.: Assessment of snow cover and surface albedo in the ECHAM5 general circulation model, J. Clim., 19, 3828–3843, 2006.

Roesch, A., Wild, M., Gilgen, H., and Ohmura, A.: A new snow cover fraction parameterization for the ECHAM4 GCM, Clim. Dyn., 17, 933–946, 2001.

Roth, T. R. and Nolin, A. W.: Characterizing maritime snow canopy interception in forested mountains, Water Resour. Res., 55, https://doi.org/10.1029/2018WR024089, 2019.

Rousseeuw, P., Croux, C., Todorov, V., Ruckstuhl, A., Salibian-Barrera, M., Verbeke, T., Koller, M., and Maechler, M.: robustbase: Basic Robust Statistics, http://CRAN.R-project.org/package=robustbase, r package version 0.92-5, 2015.

Rutter, N., Essery, R., Pomeroy, J., Altimir, N., Andreadis, K., Baker, I., Barr, A., Bartlett, P., Boone, A., Deng, H., et al.: Evaluation of forest snow processes models (SnowMIP2), Journal of Geophysical Research: Atmospheres, 114, 2009.

Satterlund, D. R. and Haupt, H. F.: Snow catch by conifer crowns, Water Resour. Res., 3, 1035–1039, https://doi.org/10.1029/WR003i004p01035, 1967.

Schmidt, R. A. and Gluns, D. R.: Snowfall interception on branches of three conifer species, Can. J. For. Res., 21, 1262–1269, 1991.

Sicart, J. E., Essery, R. L. H., Pomeroy, J. W., Hardy, J., Link, T., and Marks, D.: A sensitivity study of daytime net radiation during snowmelt to forest canopy and atmospheric conditions, J. Hydrometeorol., 5, 774–784, 2004.

Siegel, R. and Howell, J. R.: Thermal Radiation Heat Transfer, Hemisphere Publishing Corp., 1978.

Storck, P. and Lettenmaier, D. P.: Measurement of snow interception and canopy effects on snow accumulation and m elt in a mountainous maritime climate, Oregon, United States, Water Resour. Res., 38, https://doi.org/10.1029/2002WR001281, 2002.

Suzuki, K. and Nakai, Y.: Canopy snow influence on water and energy balances in a coniferous forest plantation in Northern Japan, J. Hydrol., 352, 126–138, 2008.

Teich, M. and Tarboton, D. G.: TW Daniels Experimental Forest (TWDEF) Lidar, HydroShare, https://doi.org/10.4211/hs.36f3314971a547bc8bc72dc60d6bd03c, 2016.

Teich, M., Giunta, A. D., Hagenmuller, P., Bebi, P., Schneebeli, M., and Jenkins, M. J.: Effects of bark beetle attacks on forest snowpack and avalanche formation – Implications for protection forest management, For. Ecol. Manage., 438, 186 – 203, https://doi.org/10.1016/j.foreco.2019.01.052, 2019.

Varhola, A., Coops, N., Weiler, M., and Moore, R. D.: Forest canopy effects on snow accumulation and ablation: An integrative review of empirical results, J. Hydrol., 392, 219–233, 2010.

Varhola, A., Frazer, G. W., Teti, P., and Coops, N. C.: Estimation of forest structure metrics relevant to hydrologic modelling using coordinate transformation of airborne laser scanning data, Hydrol. Earth Syst. Sci., 16, 3749–3766, 2012.

Vincent, L., Lejeune, Y., M, L., Boone, A., Gac, E. L., Coulaud, C., Freche, G., and Sicart, J. E.: Interception of snowfall by the trees is the main challenge for snowpack simulations under forests, in: Proceedings of the International Snow Science Workshop (ISSW), Innsbruck, Austria, pp. 705–710, http://arc.lib.montana.edu/snow-science/objects/ISSW2018_O08.4.pdf, 2018.

Webster, C. and Jonas, T.: Influence of canopy shading and snow coverage on effective albedo in a snow-dominated evergreen needleleaf forest, Remote Sens. Environ., 214, 48 – 58, 2018.

Yakir, B.: Nonparametric Tests: Kolmogorov-Smirnov and Peacock, chap. 6, pp. 103–124, John Wiley & Sons, Ltd, https://doi.org/10.1002/9781118720608.ch6, 2013.

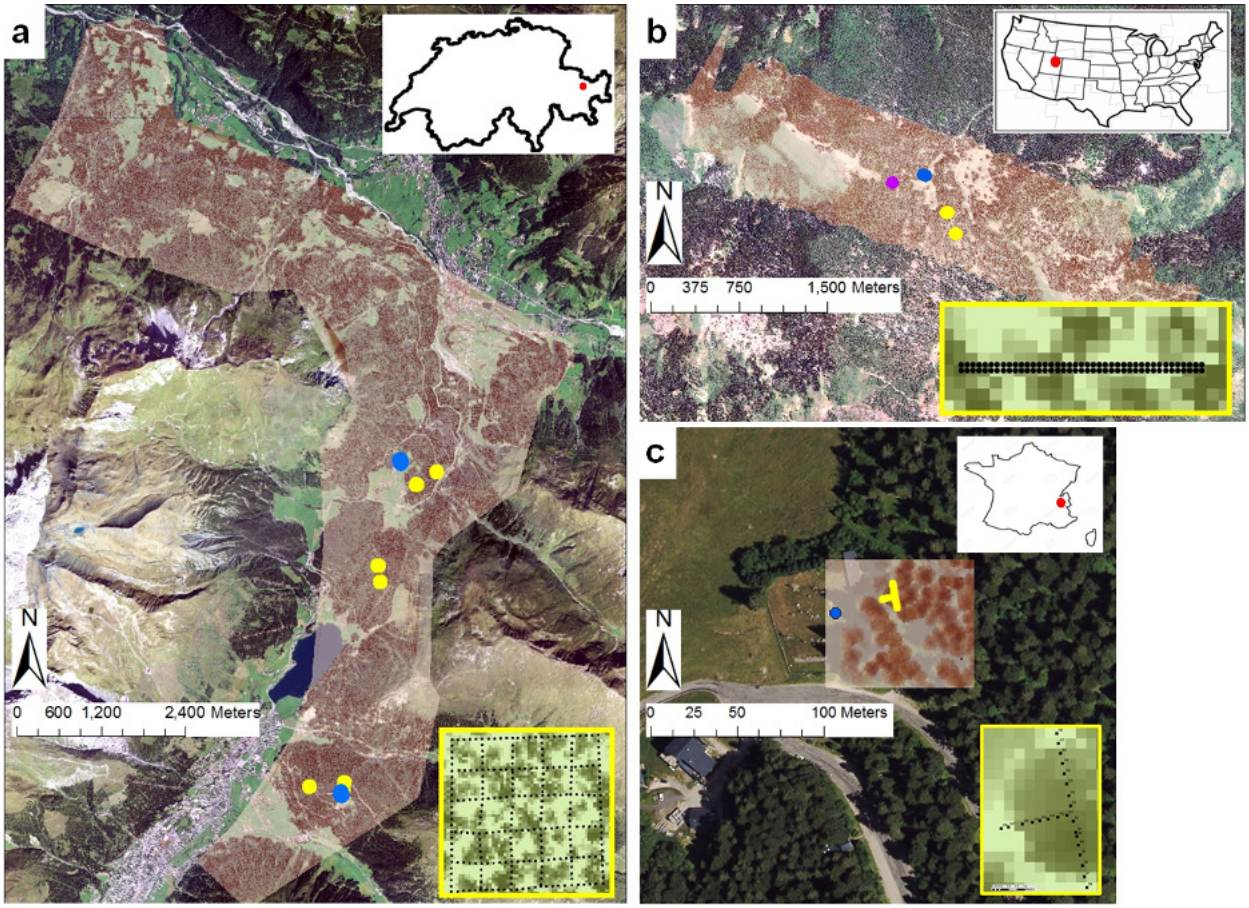

Figure 1. Extent of ~~lidar~~ LiDAR derived ~~tree DSM's~~ canopy height model (CHM) with locations of open (blue points) ~~,~~ and forested field sites (yellow points), and SNOTEL site (purple point): (a) close to Davos in the ~~Eastern~~ eastern Swiss Alps (~90 km^2; 46.78945°N, 9.79632°E), (b) in the Rocky Mountains of ~~Northern~~ northern Utah, U.S. (~~13km~~13 km^2; 41.85046°N, 111.52751°W), and (c) in the ~~Southeastern~~ southeastern French Alps at Col de Porte (~0.01 km^2; 45.29463°N, 5.76597°E). The yellow framed inlets show the respective snow depth measurement setup at the forested field sites. Underlying orthophotos were provided for the French site ~~were provided~~ by IGN (France) and for the Swiss site by Swisstopo (JA100118). For the site in the U.S. © Google Earth imagery was used.

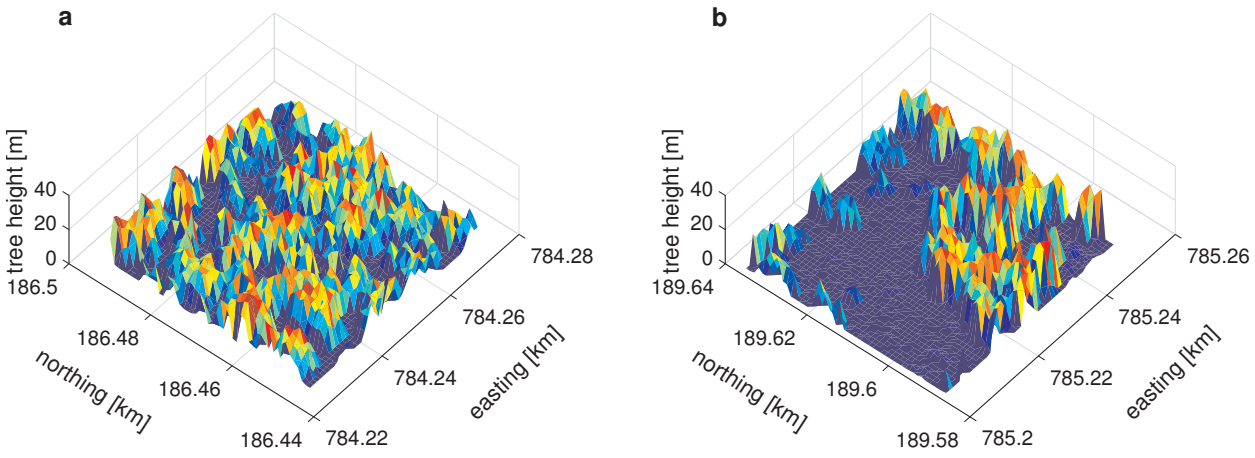

Figure 2. ~~Tree DSM's~~ Canopy height models (CHM) for two 50 x 50 m^2 field sites in 1 m grid resolution in the ~~Eastern~~ eastern Swiss Alps with (a) high canopy coverage and (b) low canopy coverage (for detailed site descriptions see Moeser et al., 2014).

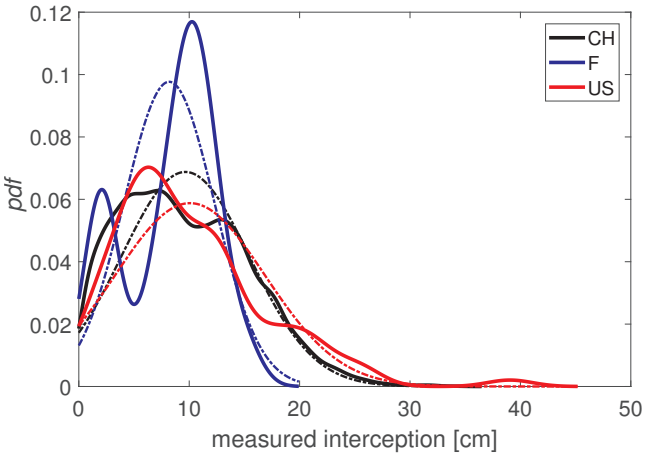

Figure 3. Probability density functions (*pdf*'s) of all individual snow depth interception measurements used for the development (Swiss (CH) data set) and for the validation of the parameterizations (French (F) and U.S. (US) data sets). The dashed lines indicate a theoretical normal *pdf* for the corresponding data set.

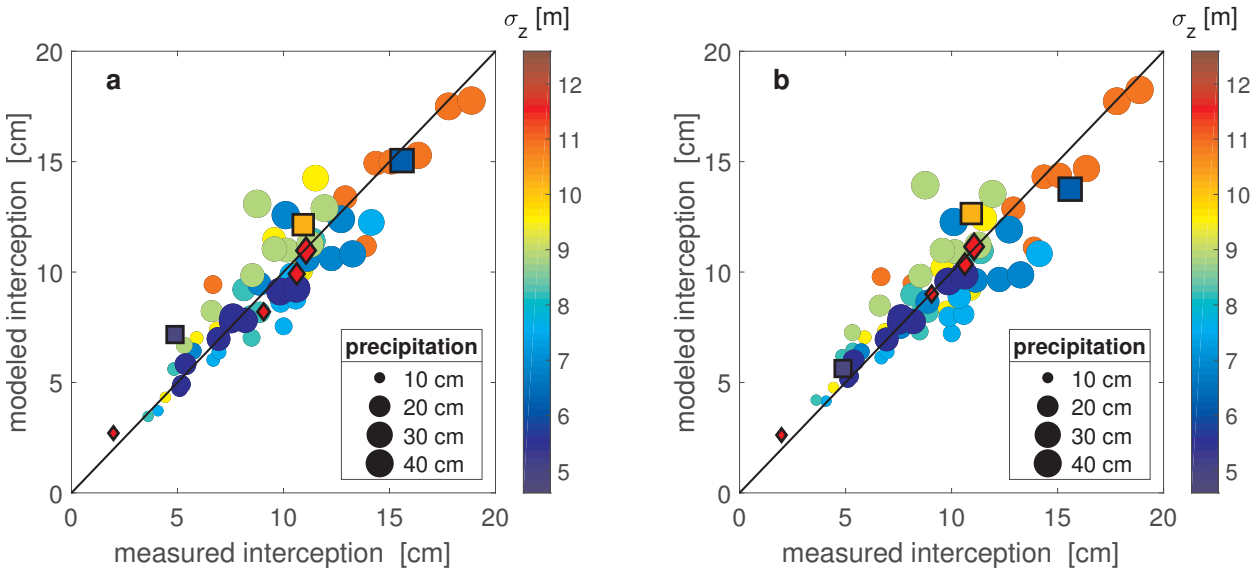

Figure 4. Measured and parameterized site means of intercepted snow depth, i.e. spatially averaged over each site and for each storm date. Parameterized using a) Eq. (2) and b) Eq. (3) as a function of site means of standard deviation of the ~~lidar~~ LiDAR DSM σ_z (in color) as well as open ~~area~~ site snow storm precipitation (size of symbols). Circles represent the development data set from Switzerland, symbols with a black border represent the validation data sets with squares for that from the U.S. and diamonds for that from France.

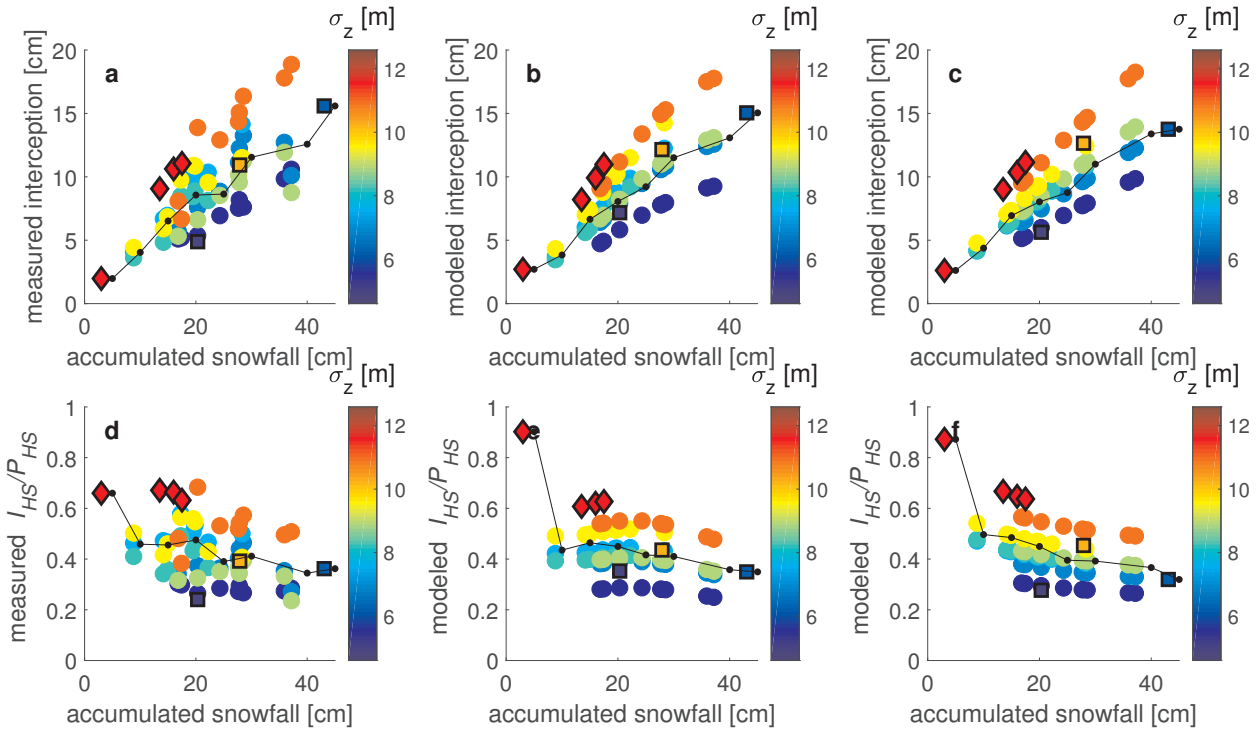

Figure 5. Snow depth interception I_{HS} (a,b,c) and interception efficiency I_{HS}/P_{HS} (d,e,f) as a function of accumulated open ~~area~~ site snow storm precipitation P_{HS} and standard deviation of the ~~lidar~~ LiDAR DSM σ_z (in color). The y-axis of the first column shows measured data, the second column shows model output with Eq. (2) and the third model output with Eq. (3). Site means for each storm event are depicted with colored circles for the development data set from Switzerland and symbols with a black border depict the validation data sets, with squares for that from the U.S. and diamonds for that from France. Storm means (in P_{HS} bins) are shown in black.

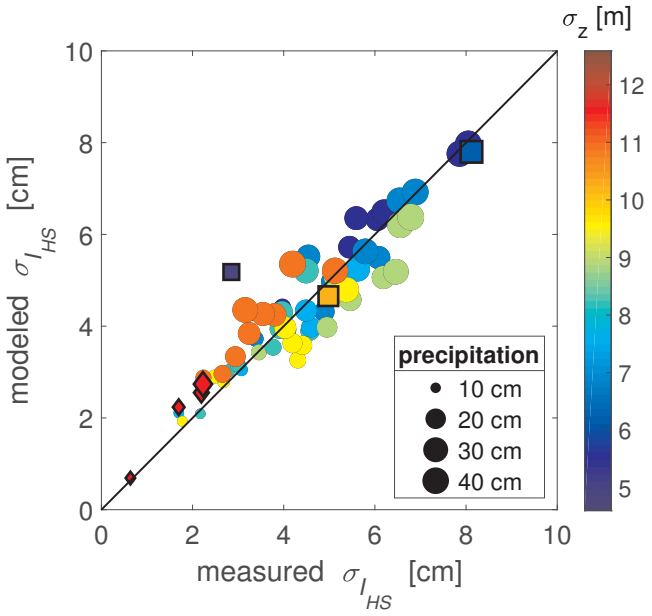

Figure 6. Measured and parameterized standard deviation of snow depth interception $\sigma_{I_{HS}}$ at each site and for each storm date. Parameterized using Eq. (4) as a function of site means of standard deviation of the ~~lidar~~ LiDAR DSM σ_z (in color) as well as open ~~area~~ site snow storm precipitation (size of symbols). Circles represent the development data set from Switzerland, symbols with a black border represent the validation data sets with squares for that from the U.S. and diamonds for that from France.

Table 1. Performance measures between measurement and parameterization of spatial-mean snow depth interception I_{HS} with (a) Eq. (2), (b) with Eq. (3)), and (c) standard deviation of snow depth interception $\sigma_{I_{HS}}$ with Eq. (4). Statistics are shown for the development data set from the ~~Eastern~~ eastern Swiss Alps (CH) and for the combined validation data set (U.S.&F).

	NRMSE	RMSE	MPE	MAE	r	K-S	$\text{NRMSE}_{\text{quant}}$
	[%]	[cm]	[%]	[cm]			[%]
a) I_{HS} (Eq. (2))							
CH	~~9.0~~ 8.7	~~1.37~~ 1.33	~~-2.0~~ -1.97	~~1.02~~ 1.01	0.92	$8.6\,10^{-2}$	~~2.2~~ 2.5
U.S.&F	~~9.4~~ 8.2	~~1.28~~ 1.12	~~-10.43~~ -10.61	~~1.11~~ 0.92	~~0.99~~ 0.97	~~$4.3\,10^{-1}$~~ $1.4\,10^{-1}$	~~9.9~~ 7.8
b) I_{HS} (Eq. (3))							
CH	10.2	1.55	~~-2.87~~ -1.65	1.15	0.89	$1.0\,10^{-1}$	~~4.9~~ 5.3
U.S.&F	~~7.6~~ 7.5	~~1.04~~ 1.03	~~-8.45~~ -7.03	~~0.78~~ 0.76	0.97	$2.9\,10^{-1}$	~~6.2~~ 5.9
c) $\sigma_{I_{HS}}$ (Eq. (4))							
CH	8.9	0.57	~~-2.04~~ -2.05	0.45	0.92	$8.6\,10^{-2}$	3.9
U.S.&F	12.7	0.95	-21.52	~~0.64~~ 0.63	0.94	$4.3\,10^{-1}$	10.4